



UNIVERSITY OF LEEDS

This is a repository copy of *Prediction of channel connectivity and fluvial style in the flood basin successions of the Upper Permian Rangal Coal Measures (Queensland)*.

White Rose Research Online URL for this paper:  
<http://eprints.whiterose.ac.uk/82575/>

Version: Accepted Version

---

**Article:**

Stuart, J, Mountney, NP, McCaffrey, WD et al. (2 more authors) (2014) Prediction of channel connectivity and fluvial style in the flood basin successions of the Upper Permian Rangal Coal Measures (Queensland). *American Association of Petroleum Geologists (AAPG) Bulletin*, 98 (2). 191 - 212. ISSN 0149-1423

<https://doi.org/10.1306/06171312088>

---

**Reuse**

Unless indicated otherwise, fulltext items are protected by copyright with all rights reserved. The copyright exception in section 29 of the Copyright, Designs and Patents Act 1988 allows the making of a single copy solely for the purpose of non-commercial research or private study within the limits of fair dealing. The publisher or other rights-holder may allow further reproduction and re-use of this version - refer to the White Rose Research Online record for this item. Where records identify the publisher as the copyright holder, users can verify any specific terms of use on the publisher's website.

**Takedown**

If you consider content in White Rose Research Online to be in breach of UK law, please notify us by emailing [eprints@whiterose.ac.uk](mailto:eprints@whiterose.ac.uk) including the URL of the record and the reason for the withdrawal request.



[eprints@whiterose.ac.uk](mailto:eprints@whiterose.ac.uk)  
<https://eprints.whiterose.ac.uk/>

1 **Prediction of channel connectivity and fluvial style in the floodbasin**  
2 **successions of the Upper Permian Rangal Coal Measures (Queensland)**

3 J.Y. Stuart<sup>1</sup>, N.P. Mountney<sup>1</sup>, W.D. McCaffrey<sup>1</sup>, S. Lang<sup>2</sup>, J.D. Collinson<sup>3</sup>

4  
5 <sup>1</sup> Fluvial Research Group, School of Earth and Environment, University of Leeds, Leeds, LS2  
6 9JT, UK

7 <sup>2</sup> Woodside Energy Ltd, Perth, WA, Australia

8 <sup>3</sup> John Collinson Consulting Limited, Delos, Knowl Wall, Beech, Staffordshire, ST4 8SE, UK

9  
10 Author for correspondence: Jen Stuart, eejs@leeds.ac.uk

11  
12 **Abstract**

13 Predicting the presence and connectivity of reservoir-quality facies in otherwise  
14 mud-prone fluvial overbank successions is important as such sandbodies can  
15 potentially provide connectivity between larger neighboring sandbodies. This  
16 paper addresses minor channelized fluvial elements (crevasse splay and  
17 distributary channels), and attempts to predict connectivity between such  
18 sandbodies in 2 interseam packages of the Upper Permian Rangal Coal  
19 measurements. Channel body percent as measured in well logs were 2% in the  
20 upper (Aries-Castor) interseam, and 17% in the lower (Castor-Pollux)  
21 interseam. Well spacing was too great to allow accurate correlation of channel  
22 bodies. The Ob River, Siberia, was used as modern analogue to supply  
23 planform geometric measurements of splay and distributary channels, so that  
24 stochastic modeling of channel bodies was possible. The resulting models  
25 demonstrated that (i) channel-body connectivity is more uniform in distributary  
26 river systems than in splay complexes; (ii) relatively good connectivity is seen in  
27 proximal positions in splays, but decreases distally from the source as channel  
28 elements diverge; (iii) connectivity tends to be greater down the axis of splays,  
29 with more isolated channel bodies occurring at the margins.

30  
31 **Keywords:** Fluvial, distributary, crevasse, secondary channel, tertiary channel,  
32 connectivity, reservoir modeling, Rangal Coal Measures, Bowen Basin, Ob  
33 River

34

## 35 **Introduction**

36 The distribution of sand bodies in fluvial overbank settings is strongly controlled  
37 by processes that dictate the style and frequency of overbank flooding  
38 (Benedetti 2003) via the breaching of levees, the generation of crevasse splays  
39 (Morozova & Smith 2000), and the development of minor distributary channels  
40 (Smith *et al.* 1989). In particular, size, longevity, spatial distribution and style of  
41 connection of splays to primary channels governs the distribution of sand-prone  
42 elements in overbank successions. The presence of reservoir-quality facies,  
43 such as secondary and tertiary splay and distributary channel deposits, in  
44 otherwise mud-prone fluvial overbank successions may provide significant  
45 connectivity between neighboring major channel elements in avulsion-prone  
46 channel belts, as in the Westphalian Coal Measures, Durham, UK (Fielding,  
47 1986).

48

49 Although determination of three-dimensional sedimentary architecture and  
50 overbank connectivity is crucial for reservoir prediction in low net:gross  
51 floodplain settings, the typical km-scale well spacing in some hydrocarbon fields  
52 is too great and the total number of wells too few for the development of the  
53 appropriate predictive models. Likewise tertiary splay and minor distributary  
54 channel elements  $\leq 3$  m thickness – Avenell 1998) are typically below the  
55 vertical resolution of seismic data (Bridge & Tye 2000; Ethridge & Schumm  
56 2007), and their presence cannot be ascertained, nor their impact on  
57 connectivity inferred, from such data.

58

59 In low-accommodation fluvial settings, sand-prone channel elements are  
60 preferentially preserved as stacked and overlapping multi-story and multi-lateral  
61 bodies, whereas in higher accommodation settings, mud-prone overbank  
62 elements have greater preservation potential and neighboring channel bodies  
63 tend to be spatially isolated (Bristow & Best 1993). An increased rate of  
64 accommodation creation is commonly attributed to one or more of the following  
65 driving mechanisms: (1) high rates of basin subsidence such as encountered in  
66 many foreland basin settings (e.g. Marenessi *et al.* 2005); (2) base-level rise  
67 (Bristow *et al.* 1999; Bourquin *et al.* 2006) Most systems are governed by a  
68 combination of these factors, although one may be dominant (Ethridge *et al.*  
69 1998).

70

71 Facies associations routinely identified in low net:gross, relatively high-  
72 accommodation fluvial overbank settings include those associated with mires,  
73 levees, secondary and tertiary distributary channels, and splays and splay  
74 complexes, including those composed of multiple tertiary splay channels, as  
75 well as finer-grained units: floodplain-lake fills and floodplain fines, including  
76 palaeosols (Smith & Pérez-Arlucea 1994; Jorgensen & Fielding 1996; Cazanagli  
77 & Smith 1998; Farrell 2001). Figure 1 illustrates the typical architecture and  
78 internal facies make-up of these depositional elements. Reservoir-quality  
79 sandstones are most likely to be present in the overbank setting as networks of  
80 secondary and tertiary channel elements, the accumulated deposits of which  
81 typically attain thicknesses of up to a few meters, and which may form laterally  
82 extensive splay bodies over distances of several kilometers. It is, however,  
83 typically difficult to distinguish between deposits of some of the smaller-scale  
84 overbank elements, particularly when relying on core or well-logs alone for  
85 interpretation (Brierley *et al.* 1997).

86

87 The aim of this study is to demonstrate the architecture and connectivity of  
88 secondary (distributary) and tertiary (distributary and splay) channelized sand  
89 bodies in a low net:gross fluvial setting, to assess the potential for  
90 communication between reservoir-quality (sandy) elements in overbank  
91 settings. Specific objectives of this study are (i) to document criteria by which  
92 minor channelized elements can be identified on wireline logs, (ii) to quantify  
93 infill proportions and dimensions of tertiary channels, (iii) to present quantitative  
94 data on plan-view geometries of modern tertiary channel elements, and (iv) to  
95 stochastically model the predicted lateral and vertical connectivity of tertiary  
96 channels. The connectivity of such sand bodies is investigated for two  
97 interseam intervals at the South Blackwater Mine, Queensland (Fig. 2), a  
98 Permian coal-bearing floodbasin succession.

99

100 This work is significant for the following reasons: (i) current models that predict  
101 sand-body occurrence in floodbasin settings are overly simplistic and largely  
102 qualitative in nature (Bridge & Tye 2000); (ii) current approaches to estimating  
103 hydrocarbon reserves in fluvial reservoirs routinely only assess the geometry of  
104 major (primary) fluvial sand bodies (e.g. multi-storey channel complexes), and

105 this potentially underestimates the true volume by ignoring the additional  
106 significant volume associated with minor secondary and tertiary channel and  
107 splay elements; (iii) few models currently exist with which to assess the role of  
108 minor secondary and tertiary channel and splay elements in terms of their role  
109 in aiding communication and connectivity between primary channel bodies.

110

## 111 **Geological Setting**

112 The Permian Rangal Coal Measures of the Bowen Basin, at the South  
113 Blackwater Mine, Bowen Basin, Queensland (Fig. 2) are exposed in a series of  
114 open cast workings and have been penetrated by a series of shallow boreholes  
115 for which well-log and core data are available. The coal measures are  
116 widespread throughout the basin and they have been exploited through  
117 intensive open-cut mining since the 1970s (Mutton 2003). The Rangal Coal  
118 Measures form part of the fill of the Bowen Basin, which evolved – along with  
119 several other Eastern Australian Gondwanan basins – as part of the Middle-  
120 Late Palaeozoic Tasman Orogen (Fielding *et al.* 1993; Fielding 2001; Fig 3).  
121 Three pulses of sedimentation directed southwards along the basin axis  
122 occurred during the Late Permian, the last of which was responsible for the  
123 accumulation of the Wuchiapingian-Changhsingian age Rangal Coal Measures  
124 and equivalents, which represent the preserved deposits of a large scale  
125 distributary fluvial system (Fielding *et al.* 1993; Allen & Fielding 2007). The  
126 sheet-like nature of primary channel deposits formed in the Rangal Coal  
127 measures is indicative of a low-sinuosity system and the Rangal Coal Measures  
128 are considered to have formed in a broad alluvial plain setting (Fielding *et al.*  
129 1993)

130

131 At the South Blackwater Mine, the Rangal Coal Measures are preserve three  
132 mineable coal seams within the study area: Aries (A), Castor (B) and Pollux (C).  
133 Within the Rangal Coal Measures, several facies associations have been  
134 recognized by previous research. Fielding (1993) identified the following: Sheet-  
135 like sandstone channel bodies; laterally accreted, heterolithic channel bodies;  
136 proximal overbank; crevasse channel fill; floodbasin; lake floor; mire. Avenell  
137 (1998) interpreted wireline and core data as: sheet-like channel sandstone  
138 bodies (primary channel elements); heterolithic distributary channel bodies  
139 (secondary channel elements); minor crevasse channel bodies (tertiary channel

140 elements); levee; floodbasin; lacustrine and mire. Michaelsen *et al.* (2000)  
141 interpreted the interseam deposits as: trunk river channels and crevasse feeder  
142 channels; levee bank–proximal crevasse splay; distal splay–overbank; marsh;  
143 peat mire and floodbasin lake.

144

## 145 **Data and Methods**

146 The study covers a 2km<sup>2</sup> area of the South Blackwater Mine, Queensland.  
147 Detailed correlation of a subsurface part of the Rangal Coal Measures  
148 succession was undertaken using a high-density subsurface dataset of wireline  
149 logs from 63 coal exploration wells. Available well logs included, including  
150 gamma-ray (GR), density, caliper and sonic logs were utilized.

151

152 High-resolution lithologic logs were made for each well in the dataset using  
153 Oilfield Data Manager (ODM) software, primarily via the interpretation of GR  
154 and density log responses. For the purpose of lithology interpretation, GR cut-  
155 offs were defined as follows: clay/mudstone, >110 API GR; siltstone and silty  
156 sandstone, 110-90 API GR; 'clean' sandstone (>60% sand), <90 API GR  
157 (Avenell, 1998). Coal was easily identified by its distinctive signature  
158 characterized by very low GR values coincident with low density values.

159

160 After assigning lithologies to each well, architectural elements (Miall, 1985)  
161 were assigned to packages of deposits deemed to have been formed by the  
162 same processes. To help achieve this, an extended and refined lithology and  
163 facies scheme for the Rangal Coal Measures was developed from a previous  
164 core-based study at the South Blackwater Mine (Avenell 1998) and this was  
165 used as the basis for the architectural-element scheme developed in this study.  
166 Patterns in well-log curves and lithologic cycles were identified and assigned  
167 to fluvial and overbank architectural elements. Architectural elements were then  
168 correlated between subsurface wells in an attempt to characterize two-  
169 dimensional facies changes and, where possible, the likely three-dimensional  
170 sedimentary architecture and style of connectivity of secondary and tertiary  
171 fluvial channel elements considered to have arisen as a product of crevassing in  
172 a distributary system.

173

174 Where it was not possible to predict architectural-element type and extent from  
175 groups of neighboring well logs, measurements and estimates of likely plan-  
176 form geometry were made via the adoption and implementation of geometries  
177 of similar elements from analogous modern systems. Study of these modern  
178 fluvial systems involved the measurement of channel widths, lengths and  
179 sinuosities using NASA Landsat and Google Earth® imagery. These analogue  
180 data were integrated into reservoir models of the study area using  
181 Reckonnect®, a fluvial stochastic modeling software package. Reckonnect was  
182 chosen due to its ability to run multiple iterations of models in a short time  
183 period, in order to test the effect on reservoir connectivity of changing the  
184 dimensions and other parameters of the channel-element sand bodies.

185

186 Interpretations of the depositional sub-environments of the Rangal Coal  
187 Measures interseam intervals were then made based on the proportions and  
188 distributions of architectural elements observed in each of the two interseam  
189 intervals, one between the Aries (A) and Castor (B) seams, and the other  
190 between the Castor (B) and Pollux (C) seams.

191

## 192 **Architectural Elements**

193 Seven principal architectural elements have been identified in the study area  
194 between the Aries (A) and Pollux (C) seams (Fig. 4) using defined GR cut-offs  
195 for sand (<90), silty sand (90-110) and mud (>110), together with correlation of  
196 wireline log signatures between neighboring well-logs. The architectural  
197 element scheme is based on that of Avenell (1998).

198

199 (1) Secondary tributary channel elements. The wireline log character of these  
200 elements shows a sharp, erosional base, with a fining-up, blocky or bell-shaped  
201 gamma response. These deposits are <90 API GR. These elements are greater  
202 than 3 m thick and are interpreted as heterolithic distributary channel-fill deposits  
203 (Fielding *et al.* 1993). Distributary channels are typically bounded by levees, are  
204 subject to some lateral accretion, and grade laterally into finer-grained floodplain  
205 deposits (Avenell, 1998), in places causing local 'washouts' of the Castor (B)  
206 seam (Fig. 6).

207

208 (2) Tertiary crevasse channel elements. These elements have a GR of <110  
209 API GR, in a succession of <3 m-thickness sandstone. They are typically sharp-  
210 based, fining-up to clayey, silty sand. The overall log signature is blocky or bell-  
211 shaped. Laterally more extensive tertiary channel elements are interpreted as  
212 those of mature crevasse channels, analogous to the stage 3 splay channels of  
213 Smith *et al.* (1989). Less extensive, poorly developed tertiary channel elements  
214 are interpreted as immature or abruptly abandoned splay channels of a stage 1  
215 or stage 2 crevasse splay (Smith *et al.* 1989).

216

217 (3) Channel-margin (including levee) and lake-margin elements. Channel-  
218 margin deposits form the finer-grained equivalent to adjoining channelized  
219 deposits. They typically exhibit fine-grained (alternating high and low GR) log  
220 patterns, corresponding to interbedded sandstones, siltstones and clay drapes.  
221 Lake-margin deposits routinely exhibit coarsening-up, progradational log  
222 patterns, but are difficult to distinguish from levee channel-margin deposits  
223 where observed in wireline borehole logs alone.

224

225 (4) Proximal- to medial-floodplain elements. Deposits of these elements consist  
226 of interlaminated sandstone, siltstone and clay-rich partings, with a highly  
227 variable log pattern attributed to splays and flooding.

228

229 (5) Distal floodplain elements. Deposits of these elements are characterized by  
230 laminated siltstones and mudstones, with a GR log signatures generally >110  
231 API GR. Minor sandstone intervals identified in these packages likely represent  
232 the distal deposits of crevasse splays.

233

234 (6) Floodplain lake and frequently inundated floodplain elements. These  
235 deposits of interlaminated claystones, mudstones and silty-mudstones, with rare  
236 lenses of siltstone and sandstone, have GR log readings generally >110 GR  
237 API. They are indicative of a system subject to seasonal flooding.

238

239 (7) Mire elements. Within these deposits, a blocky, low GR-log signature is  
240 indicative of coals. This 'blocky' GR response, together with a low DENL  
241 response distinguishes coal from sandstone. These deposits constitute coal  
242 seams and carbonaceous shales formed in peat mires.



243

244 Thick and sheet-like primary channel-fill elements are not encountered in the  
245 interseam deposits of the study area, though such bodies are identified from  
246 some wells beneath the C seam. Most wells stopped at or just beneath the C  
247 seam, so correlation of these extensive sand-prone elements has not been  
248 possible.

249

## 250 **Correlation**

251 Figure 5 details a typical subsurface well correlation, taken from the northeast of  
252 the study area (see inset map for location). The correlation utilizes caliper,  
253 gamma-ray and density wireline logs to identify the three major coal seams  
254 present in the studied interval, to interpret the interseam lithology, and to  
255 interpret the architectural elements present in the interseams. Fence diagrams  
256 collating key correlation panels were constructed to demonstrate the three-  
257 dimensional architecture of the interseam deposits (Fig. 6) and to identify key  
258 areas of secondary and tertiary fluvial channel deposition.

259

## 260 **Element Proportions**

261 Proportions of the A-B, and B-C interseam intervals infilled by each architectural  
262 element were measured from their thicknesses in each interpreted well log (Fig.  
263 7). Net:gross was calculated for each interval (A-C, A-B, B-C), taking only  
264 'clean' (GR <90 API) sandstone as net. The correlation panel and fence  
265 diagram (Figs. 5 & 6) demonstrate that the B-C interseam has a greater  
266 proportion of channel elements and therefore a higher net:gross than the A-B  
267 interseam.

268

## 269 **Channel Element Thicknesses and Widths**

270 Channel-element thicknesses were determined from well logs. A frequency plot  
271 reveals the distribution of the range of channel thicknesses (Fig. 8), where  
272 frequency refers to the number of appearances in well logs. It was not possible  
273 to measure channel-element widths using the well correlation data alone  
274 because well spacing was greater than the width of the channel elements in  
275 most cases, such that estimated widths measured from correlation panels

276 effectively became a function of the well spacing rather than a true indicator of  
277 channel-body width.

278

279

## 280 **Interpretation**

### 281 **Analogue Measurements**

282 In cases where it is not possible to directly derive all the information necessary  
283 to build accurate reservoir models from available datasets, analogue data may  
284 be used to approximate the missing parameters (e.g. plan-form geometry) that  
285 cannot be determined from the primary subsurface dataset alone (Alexander,  
286 1993; Lang *et al.* 2002). For overbank depositional systems whose constituent  
287 architectural elements (e.g. floodplain and splay) are readily preserved, such as  
288 those of the Rangal Coal Measures, modern analogues must be chosen from  
289 relatively high-accommodation fluvial/fluviodeltaic settings in which extensive  
290 peat-forming processes are acting and for which frequent flooding, crevassing  
291 and deposition occurs on the floodplain.

292

293 One modern example is the Ob River, Siberia. The Ob River was selected as a  
294 suitable analog as it is set within the large-scale, continental, non-tropical peat-  
295 forming depositional system in the West Siberian Plain (Lang *et al.* 2002). The  
296 Ob River has a very large primary channel (fig. 9). However it is the numerous  
297 secondary and tertiary channels, running roughly perpendicular to the primary  
298 channel, that have been identified as likely modern equivalents of the  
299 distributary and splay channels present at the time of deposition of the Rangal  
300 Coal Measures at the location of the South Blackwater Mine (Lang *et al.* 2002).  
301 This analogue is used to link surface geomorphology to subsurface  
302 sedimentology in the South Blackwater Mine dataset. The Ob River distributary  
303 system floods seasonally (Fig. 9a), with floods emanating from breaches in  
304 levees that result in widespread crevassing, the generation and maintenance of  
305 secondary and tertiary distributary channels (Fig. 9b) during spring floods. As  
306 the floods dry during summer months, the receding water leaves abundant  
307 floodplain lakes across the floodplain (Lang *et al.* 2002). Figure 9c illustrates a  
308 typical crevasse splay complex of the Ob River, and this is considered to be  
309 similar in both scale and morphology to those envisaged for the South

310 Blackwater study succession, based on the similarity in scale of the various  
311 architectural elements known from the two systems.

312

313 Measurement of the dimensions of the planform geometries of tertiary channels  
314 of the Ob River (both splay and distributary), including width, length and  
315 sinuosity, were taken from Google Earth aerial photographs (Table 1). Mean  
316 sinuosity (1.16) and width (41.60 m) of splay channels (N = 43) was less than  
317 that of the distributary tertiary channels (sinuosity = 1.27; width = 59.75 m, N =  
318 24).

319

## 320 **Modeling**

321 The tertiary channels in the Ob River record little evidence for significant lateral  
322 migration via the accretion of point-bar deposits, so preserved sediment  
323 geometries assumed to be similar to those on the surface. Measurements of  
324 the widths and sinuosities of active channels from the Ob River analogue were  
325 therefore used in combination with the subsurface data, to derive estimates of  
326 likely infill proportions and channel thickness:width relationships for the Rangal  
327 Coal Measures. These were in turn used to define input ranges for stochastic  
328 models of the interseams made using Reckconnect (fluvial stochastic modeling  
329 software).

330

331 Reckconnect is a stochastic, object-based model that quickly models channel  
332 bodies to assess the effect of changing channel body dimensions and  
333 distributions on connectivity (Collinson & Preater). Models are created using  
334 channel body thickness and channel percentage data from wells, and geometric  
335 data (e.g. channel body width and sinuosity). Modelled output is simple, treating  
336 all channel bodies as reservoir, and all other deposits (model background) as  
337 non-reservoir. The models allow quantification of channel body connectivity, as  
338 well as connectivity to pseudo-wells.

339

340 For each model run, graphic output from a a randomly selected run was  
341 generated to illustrate the form of modeled channel geometries, and predicted  
342 style of clustering, channel connectivity (where channel connectivity by volume  
343 is defined as the mean percentage of sand connected to a random sandy point),  
344 and channel-body percentages observed in pseudo-wells. Results demonstrate

345 potential well connectivity to sand bodies in the model, where well connectivity  
346 is defined as the probability (%) that pseudo-wells are connected by a  
347 continuous sandy path (Fig. 10a).

348

349

350 Reconnect is not suitable for modeling two types of channel simultaneously  
351 (i.e. secondary and tertiary channels), and therefore models were built to  
352 represent the distribution of tertiary channels, which make up a greater  
353 proportion of interseam infill. In the A-B (Aries-Castor) interseam, infill by minor  
354 channels is 2% by tertiary channels and <1% by secondary channels. In the B-  
355 C (Castor-Pollux) interseam, the bias towards tertiary channels is greater with  
356 17% infill by tertiary channels and 2% by secondary channels.

357 As both splay and distributary channels are identified in the South Blackwater  
358 Mine (Avenell, 1998) and in the Ob River (Fig. 9), both of these fluvial styles  
359 were modeled for the interseam deposits. Figures 10-12 show random  
360 replications from modeling runs conducted with 100 replications in each run. As  
361 well as the graphic output, Reconnect also generates statistics covering  
362 channel proportion, channel connectivity and sand connectivity to pseudo-wells  
363 for each modeling run, summaries of which are given in tables 2-4. Model inputs  
364 are listed in Tables 2a, 3a and 4a.

365

366 The sand-poor A-B interseam was modeled with a splay (fan-like) geometry  
367 (Fig. 10b), whereby all modeled channels were forced to originate from a single  
368 point; this is the most likely arrangement to account for the low proportion of  
369 channel-infill and interpreted poor channel network development within the  
370 modeled interseam volume. The B-C interseam was modeled with both splay  
371 and distributary geometries, the latter type being characterized by channels that  
372 have no fixed point of origin within the model.

373

374 Due to the low proportion (2%) of channel-body infill in the A-B interval, very few  
375 channel bodies are modeled, and the majority (on average 87%) of those that  
376 are present are isolated (i.e. are not in communication with another channel  
377 body within the modeled interval) (Fig. 10b). Channel-body connectivity was low  
378 across most of the model (mean channel-body connectivity = 13%). The  
379 pseudo-wells demonstrate that, in both proximal and distal locations, wells are

380 likely only to intersect isolated (i.e. non-clustered) channel bodies, if any, with  
381 the mean well connectivity being only 1.9%.

382

383 The B-C interseam, when modeled as a crevasse splay complex (Fig. 11),  
384 displayed the following features compared to the model for the A-B interseam:  
385 greater overall channel-body percentage (17%), greater mean channel-body  
386 thickness (1.59 m), which resulted in higher mean connectivity of channel  
387 bodies (22%) such that they formed multiple clusters of connected channel  
388 bodies. As expected in a splay, channel-body connectivity decreased distally  
389 and away from the axis of the splay, with isolated channel bodies more  
390 commonly occurring towards the splay margins. Figure 11 demonstrates a  
391 representative output from the B-C (splay) modeling runs: pseudo-wells  
392 demonstrate that, for a proximal location, it is possible for wells to intersect  
393 almost all of the channel clusters, whereas for distal locations, a well will  
394 intersect fewer channel bodies, the majority of which are likely to be isolated.  
395 Mean well connectivity is 46%: i.e. by intersecting channel clusters, a single well  
396 would be predicted, on average, to be in communication with 46% of the  
397 channel bodies modeled.

398

399 When modeled as a distributary system – i.e. where channels have no fixed  
400 point of origin (Fig. 12) – the B-C interseam displayed the following features:  
401 distributary tertiary channels were modeled with greater widths and sinuosities  
402 than crevasse-splay channels, using width and sinuosity measurements  
403 provided from the Ob River (Table 1). This resulted in greater amalgamation  
404 and stacking of channel bodies and generated fewer but larger channel-body  
405 clusters, yielding an average channel-body connectivity of 54% by volume.  
406 Channel-body connectivity was distributed more randomly across the modeled  
407 interval compared to that predicted by models of the interval that used a splay-  
408 type geometry (Fig. 12, '% channels connected' inset figure). As a result,  
409 pseudo-wells were, on average, likely to intersect all of the channel clusters,  
410 yielding a mean well connectivity of 79.8%.

411

## 412 **Discussion**

### 413 **Depositional Models**

414 Typical plan-form geometries of tertiary channel-body assemblages – i.e.  
415 elements generated in splay complexes and distributary channel settings – from  
416 the Ob River have been combined with channel body distributions resulting from  
417 the random replications of stochastic modeling runs in order to propose three-  
418 dimensional architectural models of the A-B (Aries-Castor) and B-C (Castor-  
419 Pollux) interseam deposits of the Rangal Coal Measures succession.

420

421 **Upper (A-B interseam) interval:** The A-B interseam is a poorly developed  
422 crevasse splay complex, with few, poorly connected channel bodies in a very  
423 low net:gross, distal floodplain setting (Fig. 13). Negligible connectivity is  
424 predicted for this interval. Channel bodies are mostly immature, being poorly  
425 developed, thin and isolated. The inset well-logs taken from the South  
426 Blackwater Mine dataset demonstrate typical successions from the interval (Fig.  
427 13). Channel bodies present are interpreted as small scale-tertiary channels  
428 that abruptly grade laterally into channel-margin levee and lake-margin  
429 deposits.

430

431 The difference in fluvial style between A-B interseam deposits and the lower  
432 B-C interseam deposits may be attributed to a number of factors. The deposits  
433 could have formed during an episode of increased rate of accommodation  
434 creation, resulting in drowning of mires, splays and more medial floodplain  
435 deposits, thereby preferentially preserving distal floodplain deposits, rather than  
436 primary channel deposits.

437

438 **Lower (B-C interseam) interval:** The B-C (Castor-Pollux) interseam can be  
439 interpreted as large, well-developed crevasse splay complex (Fig. 14), which  
440 evolved over time to preserve a network of interconnected splay-channel  
441 elements in a medial floodplain setting (similar to those seen in the Ob River).  
442 Connectivity likely exhibits a large spatial variation, being significantly greater in  
443 proximal positions, where channels are more closely clustered adjacent to the  
444 source of the splay. The inset wireline well logs demonstrate typical medial and  
445 distal successions from the interval (Fig. 14).

446

447 The B-C interseam can alternatively be interpreted as a complex assemblage of  
448 bifurcating, meandering distributary channel bodies (Fig. 15). Distributary

449 channel bodies interpreted from this part of the succession are considered to be  
450 of low sinuosity (Fielding *et al.* 1993). A network of distributary-channel  
451 elements will have a higher overall connectivity, and a more random distribution  
452 of connectivity than channel elements modeled as a crevasse-splay  
453 morphology.

454

455 A network of distributary channels originating at various points along a reach of  
456 the larger primary channel might explain the large number of channel bodies  
457 observed in the subsurface succession, in contrast to the relatively channel-  
458 poor overlying A-B interseam. The inset well-logs demonstrate successions  
459 predicted at various locations in such a system. Deposits in the South  
460 Blackwater Mine dataset generally grade laterally from channel element, to  
461 channel-margin element, to medial floodplain element, and locally to distal  
462 floodplain element (Avenell 1998). The B-C interseam is considered to be  
463 closely analogous to the floodplain morphology of the modern Ob River.

464

#### 465 **Limitations of data**

466 The principal limitation for this study is the limited lateral extent of the data,  
467 leading to uncertainty as to where the data is situated in the overall depositional  
468 system, and how representative of that system it is. A single splay in the Ob  
469 River (Fig. 9c) is 4000 m by 5000 m, yet the entire study area at South  
470 Blackwater Mine measures only 1000 m by 2000 m. Thus, the predictions of  
471 subsurface fluvial architecture arising from this study could represent only a  
472 small portion of a much larger distributary system, so care must be taken when  
473 extrapolating interpretations made from such small sub-sections of what is  
474 overall a much larger fluvial system. This may explain the contrasting styles of  
475 deposition interpreted in the A-B and B-C interseams, including the observed  
476 differences in the proportions of overall channel bodies – 2% versus 17%,  
477 respectively.

478

479

480 Although apparently an extremely low net:gross interval, with negligible  
481 reservoir potential, the A-B interseam examined in the study area might  
482 represent a low net:gross fluvio-lacustrine environment located in a floodplain  
483 setting, at a stratigraphic level which overall has a greater reservoir potential

484 elsewhere within the larger system. Analysis of a larger dataset from a wider  
485 spatial area could provide additional insight into the regional variability of such  
486 systems.

487

## 488 **Conclusions**

489 Subsurface datasets, even those of relatively high resolution such as the closely  
490 spaced coal mine wells of the South Blackwater Mine, may still not provide data  
491 of sufficient density of coverage to accurately resolve small-scale (tertiary)  
492 channel-element dimensions in floodbasin settings. Where the spacing of  
493 subsurface wells is greater than the mean width of any channel elements  
494 present, modern analogues can be a useful tool in supplementing the primary  
495 dataset to yield information regarding likely analogous plan-form geometries.

496

497 Simple models created using Reckonnect reservoir modeling software  
498 demonstrate some characteristic features of channel connectivity in small-scale  
499 distributary fluvial systems developed in floodbasin settings, such as those of  
500 the Rangal Coal Measures succession: (i) channel-body connectivity is more  
501 uniform in distributary river systems than in splay complexes; (ii) relatively good  
502 connectivity is seen in proximal positions in splays, but decreases distally from  
503 the source as channel elements diverge; (iii) connectivity tends to be greater  
504 down the axis of splays, with more isolated channel bodies occurring at the  
505 margins.

506

507 Good connectivity between channel bodies is expected in some cases (e.g. in  
508 the B-C interseam, which has a 17% channel proportion). However, where  
509 channel percentage is very low, as in the A-B interseam, connectivity between  
510 channel bodies is negligible. It is therefore vital to accurately constrain the  
511 proportions of infill by each architectural element in the system, in order to  
512 produce models with realistic channel-body distributions and connectivities.

513

514 Care must be taken when extrapolating findings from small datasets to a larger  
515 scale, as a small dataset may provide a biased, non-representative  
516 representation of the subsurface at a regional scale. This may be of particular  
517 relevance in petroleum exploration, where seismic datasets typically cannot  
518 resolve small-scale channel elements, and where well data are sparse,



519 potentially leading to biased estimations of architectural-element proportions,  
520 especially where inappropriate analogues have been used to provide  
521 supplementary data.

522

## 523 **Acknowledgments**

524 This work was funded through the sponsorship of the Fluvial Research Group at  
525 the University of Leeds by Areva, BHP Billiton, ConocoPhillips, Nexen, Saudi  
526 Aramco, Shell and Woodside. Open-release subsurface data from the Rangal  
527 Coal Measures (released for Avenell in 1998 by BHP) were provided by  
528 Woodside. This work has benefited from an earlier study by Avenell (1998), the  
529 borehole dataset being a subset of that used by Avenell. Woodside provided  
530 logistical support to assist in gaining access to the data. The authors thank John  
531 Preater for the provision of Reckonnect® modeling software.

532

## 533 **References**

- 534 Alexander, J., 1993, A discussion on the use of analogues for reservoir geology:  
535 Geological Society Special Publications, v. 69, p. 175-194.
- 536 Allen, J. P., and C. R. Fielding, 2007, Sequence architecture within a low-  
537 accommodation setting: An example from the Permian of the Galilee and  
538 Bowen basins, Queensland, Australia: AAPG Bulletin v. 91, p. 1503-  
539 1539.
- 540 Avenell, L. C., 1998, The South Blackwater Reservoir Analogue Project  
541 (Thesis), Queensland University of Technology, Brisbane, 70 p.
- 542 Benedetti, M. M., 2003. Controls on overbank deposition in the Upper  
543 Mississippi River. *Geomorphology*, v. 56 (3-4), p. 271-290.
- 544 Bourquin, S., S. Peron, and M. Durand, 2006, Lower Triassic sequence  
545 stratigraphy of the western part of the Germanic Basin (west of Black  
546 Forest): Fluvial system evolution through time and space: *Sedimentary  
547 Geology*, v. 186, p. 187-211.
- 548 Bridge, J. S., and R. S. Tye, 2000, Interpreting the Dimensions of Ancient  
549 Fluvial Channel Bars, Channels, and Channel Belts from Wireline-Logs  
550 and Cores: AAPG Bulletin, v. 84, p. 1205-1228.
- 551 Brierley, G. J., R. J. Ferguson, and K. J. Woolfe, 1997, What is a fluvial levee?:  
552 *Sedimentary Geology*, v. 114, p. 1-9.

- 553 Bristow, C. S., and J. L. Best, 1993, Braided rivers: perspectives and problems:  
554 Geological Society Special Publications, v. 75, p. 1-11.
- 555 Bristow, Skelly, and Ethridge, 1999, Crevasse splays from the rapidly  
556 aggrading, sand-bed, braided Niobrara River, Nebraska: effect of base-  
557 level rise: *Sedimentology*, v. 46, p. 1029-1047.
- 558 Cazanacli, D. & N. D., Smith, 1998. A study of morphology and texture of  
559 natural levees - Cumberland Marshes, Saskatchewan, Canada.  
560 *Geomorphology*, v. 25 (1-2), p. 43-55.
- 561 Collinson, J. & J. Preater, Reckonnect® Connectivity modelling software:  
562 <http://www.reckonnect-software.com/>
- 563 Ethridge, F. G., and S. A. Schumm, 2007, Fluvial seismic geomorphology: a  
564 view from the surface: Geological Society, London, Special Publications,  
565 v. 277, p. 205-222.
- 566 Ethridge, F. G., L. J. Wood, and S. A. Schumm, 1998, Cyclic variables  
567 controlling fluvial sequence development: Problems and Perspectives:  
568 SEPM Special Publication, v. 59, p. 17-29.
- 569 Farrell. K. M., 2001, Geomorphology, facies architecture, and high-resolution,  
570 non-marine sequence stratigraphy in avulsion deposits, Cumberland  
571 Marshes, Saskatchewan. *Sedimentary Geology*, v. 139 p. 93-150.
- 572 Fielding, C. R., 1986, Fluvial channel and overbank deposits from the  
573 Westphalian of the Durham coalfield, NE England: *Sedimentology*, v. 33,  
574 p. 119-140.
- 575 Fielding, C. R., A. J. Falkner, and S. G. Scott, 1993, Fluvial response to  
576 foreland basin overfilling; the Late Permian Rangal Coal Measures in the  
577 Bowen Basin, Queensland, Australia: *Sedimentary Geology*, v. 85, p.  
578 475-497.
- 579 Lang, S. C., J. Kassar, J. Benson, C. Grasso, T. Hicks, N. Hall, and C. Avenell,  
580 2002, Reservoir Characterisation of Fluvial, Lacustrine and Deltaic  
581 Successions - Applications of Modern and Ancient Geological  
582 Analogues: Proceedings, Indonesian Petroleum Association, v. 1, p. 557-  
583 578.
- 584 Marenessi, S. A., C. O. Limarino, A. Tripaldi, and L. I. Net, 2005, Fluvial  
585 systems variations in the Rio Leona Formation: Tectonic and eustatic  
586 controls on the Oligocene evolution of the Austral (Magallanes) Basin,

587 southernmost Argentina: *Journal of South American Earth Sciences*, v.  
588 19, p. 359-372.

589 Miall, A. D., 1985, *Architectural-Element Analysis: A New Method of Facies*  
590 *Analysis Applied to Fluvial Deposits: Earth-Science Reviews*, v. 22, p.  
591 261-308.

592 Michaelsen, P., R. A. Henderson, P. J. Crosdale, and S. O. Mikkelsen, 2000,  
593 *Facies Architecture and Depositional Dynamics of the Upper Permian*  
594 *Rangal Coal Measures, Bowen Basin, Australia: Journal of Sedimentary*  
595 *Research*, v. 70, p. 879-895.

596 Morozova, G. S., and N. D. Smith, 2000, *Holocene avulsion styles and*  
597 *sedimentation patterns of the Saskatchewan River, Cumberland*  
598 *Marshes, Canada: Sedimentary Geology*, v. 130, p. 81-105.

599 Mutton, A. J. (Compiler), 2003, *Queensland Coals 14th Edition*, Queensland  
600 Department of Natural Resources and Mines. Smith, N. D., T. A. Cross,  
601 J. P. Dufficy, and S. R. Clough, 1989, *Anatomy of an avulsion:*  
602 *Sedimentology*, v. 36, p. 1-23.

603 Smith, N. D., and M. Pérez-Arlucea, 1994, *Fine-Grained Splay Deposition in the*  
604 *Avulsion Belt of the Lower Saskatchewan River, Canada: Journal of*  
605 *Sedimentary Research*, v. 64B, p. 159-168.

606 Smith, N. D., T. A. Cross, J. P. Dufficy, and S. R. Clough, 1989. *Anatomy of an*  
607 *avulsion. Sedimentology*, v36 (1), p. 1-23.

608

## Table Captions

Table 1. Summary of tertiary channel dimensions from the Ob River, Siberia.

Table 2. A-B interseam modeling results for a splay-type geometry.

Table 3. B-C interseam modeling results for a splay-type geometry.

Table 4. B-C interseam modeling results for a distributary-type geometry.

## Figure Captions

**Fig. 1.** Schematic diagram illustrating the typical facies associations and architectural elements encountered in a low net:gross fluvial overbank environment.

**Fig. 2.** Location of the Bowen Basin and South Blackwater Mine. Adapted from Allen & Fielding (2007) and Fielding et al. (1993).

**Fig. 3.** Tectonostratigraphic chart detailing tectonic phases in the Bowen Basin region and their relationship to corresponding formations. Rangal Coal Measures are highlighted. Adapted from Allen & Fielding (2007).

**Fig. 4.** Architectural element scheme of the fluvial and overbank deposits of the Rangal Coal Measures present in the interseam packages of the South Blackwater Mine, Queensland (Adapted in part from Avenell 1998). Lithologies and architectural elements assigned using gamma-ray (GRDE) and density (DENL) logs.

**Fig. 5.** Correlation panel from the NE of the study area (location circled on the inset map), demonstrating negligible net:gross A-B interseam and low-to-moderate net:gross B-C interseam, where both tertiary and secondary channels are present. Location of the correlation is shown in the inset map, as is the location of the fence diagram (Fig. 6). Wireline log abbreviations: GRDE (gamma ray, API units), DENL (density), CADE (caliper).

**Fig. 6.** Fence diagram demonstrating presumed 3D spatial geometry of elements. Laterally continuous fine-grained floodplain deposits are accurately correlated. Well spacing was too wide (50 m to 250 m) to accurately correlate tertiary channels, which globally are typically less than 250m width (Gibling 2006). Attempts to correlate individual channel bodies has lead to some unrealistic correlations. Negligible net: gross in A-B interseam, 20% net:gross in B-C interseam.

**Fig. 7.** Well logs provided proportions of infill by each architectural element in both (a) the Aries-Castor (A-B) interseam and (b) the Castor-Pollux (B-C) interseam. Proportions measured by thickness of occurrence in studied well logs. The A-B interseam is dominated by distal deposits, with only 2% tertiary channel infill, whereas the B-C interseam is dominated by medial deposits, with 17% tertiary channel infill.

**Fig. 8.** Tertiary channel element thickness data taken from well logs in both the A-B and B-C interseams.

**Fig. 9.** (a) Overview image of the Ob River, Siberia. This large-scale, distributary system has a up to 40 km-wide floodplain. The primary channel is low sinuosity, over 1 km wide, and numerous secondary distributary and tertiary (distributary and crevasse) channels are present. (b) A typical crevasse splay from the Ob River, Siberia, measuring 5 km in length. Green areas represent the raised crevasse complex, and tertiary channel levees. Dark areas of the floodplain are inundated by spring flood waters. (c) Secondary and tertiary distributary channels in the Ob River, Siberia. Channels exhibit a range of sinuosities and bifurcations are common. Splay complexes exhibit a fractal nature, with mini 'splays' often originating from larger splay complexes and tertiary channels.

**Fig. 10.** (a) Schematic diagram explaining the graphic outputs of Reckconnect modeling runs used in Figs. 10b-12. The graphic output represents one random replication out of 100 iterations made in each modeling run. (b) Graphic output of a random replication from a Reckconnect modeling run, representing the A-B interseam, with a splay geometry. With only 2% channel infill in the interval, the cross-section shows very few channels, the majority of which are isolated (shown in

grey). The depth slice demonstrates channel orientations and geometries (depth slice location shown in light green on the cross-section). The connectivity scale can be used to interpret the channel connectivity and channel percentage outputs: Channel connectivity is negligible across most of the model. Mean channel connectivity is 11%; i.e. 11% of the 2% of the model infilled by channel bodies is connected. In this scenario, only 0.02% of the modeled interval is represented by reservoir-quality sand bodies that are in some way connected. The pseudo wells demonstrate that in both proximal and distal locations, the well is likely only to intersect isolated channels, if any. Table 2c shows the statistical output from this replication.

**Fig. 11.** Graphic output of a random replication from a Reckconnect modeling run, representing the B-C interval, with a splay geometry. The cross-section shows five main channel clusters. As expected in a crevasse splay setting, isolated (grey) channels occur most commonly towards the margins of the modeled splay complex. The depth slice demonstrates channel orientations and geometries (depth slice location shown in light green on the cross-section). The connectivity scale can be used to interpret the channel connectivity, and channel percentage outputs: Channel connectivity is highest in a proximal location and as it decreases distally, is greater along the axis of the splay than towards the outer margins. Mean channel connectivity is 20%, but is as high as 80% near the source of the splay. The pseudo-wells demonstrate that in a proximal location, it is possible to intersect almost all of the channel clusters. In a distal location, however, the well intersects fewer channels, and is likely to intersect isolated channels. Table 3c shows the statistical output from this replication.

**Fig. 12.** Graphic output of a random replication from a Reckconnect modeling run, representing the B-C interval, with a distributary geometry (i.e. the channels do not have a fixed point of origin). The cross-section shows three main channel clusters. Only a few isolated (grey) channels are present. The depth slice demonstrates channel orientations and geometries (depth slice location shown in light green on the cross-section). The connectivity scale can be used to interpret the channel connectivity, and channel percentage outputs: The more random orientation of channels allows greater connectivity between channel bodies (45% of channel

bodies are connected). There is also a more random spread of connectivities and channel percentages in the model. Mean channel connectivity is 45%, but is as high as 90-100% in some areas. The pseudo-well demonstrates that it is possible to intersect the two largest channel clusters, so that the pseudo well is in communication with 77% of the channel bodies. Table 4c shows the statistical output from this replication.

**Fig. 13.** Simplified 3D architectural model of the Aries [A] - Castor [B] seam interval, incorporating planform geometries from modern analogues, and channel element dimensions and distributions from Reckconnect modeling. Analysis of wireline-log data indicates that silty mudstones, mudstones and claystones dominate the interval; typical of distal floodplain and lacustrine deposits. The inset logs are examples of proximal and distal logs from the A-B interseam. Tertiary channel elements present in the interval tend to be isolated, and are interpreted as small-scale, crevasse splay channels, bordered by leveed channel-margin deposits. Channelised elements are attributed to the distributary fluvial system that was responsible for drowning out the B seam peat mire environment.

**Fig. 14.** Simplified 3D architectural diagram for the B-C interseam, with tertiary channels present as leveed crevasse splay channels. The diagram incorporates planform geometries of the Ob River modern analogue with channel distributions inline with model outputs from Reckconnect. Medial floodplain deposits are dominantly preserved. Isolated channels tend towards the margins of the splay, with connectivity decreasing distally from the splay source. There is overlapping of channels (as demonstrated by the BC1 modeling run, Fig. 11). The connectivity between channel bodies may be further enhanced by potential connectivity through fine sand or silty-sand splay stacks. The inset well log sections illustrate anticipated proximal and distal well logs for such a splay-based system.

**Fig. 15.** Simplified 3D architectural diagram for the B-C interseam, with tertiary channels present as leveed, meandering, bifurcating distributary channels. The diagram incorporates planform geometries of the Ob River modern analogue with channel distributions inline with model outputs from Reckconnect. Medial floodplain deposits are dominantly preserved. Some channels are isolated, however

connectivity is good where channels overlap. The inset well log sections illustrates relatively high net:gross areas anticipated within the system.



**Table 1.** Summary of tertiary channel dimensions from the Ob River, Siberia

<b>Channel Type</b>	<b>Mean Width (m)</b>	<b>Mean Length A (km)</b>	<b>Mean Sinuosity</b>
Distributary Tertiary	59.75	11.12	1.27
Splay 1 Tertiary	50.95	5.85	1.23
Splay 2 Tertiary	41.14	1.83	1.06
Splay 3 Tertiary	34.40	3.92	1.18
Splay 4 Tertiary	34.38	2.22	1.21
Splay 5 Tertiary	32.57	1.81	1.12
All Splay Tertiary	41.60	3.13	1.16

**Table 2.** A-B interseam modeling results, modeled with a splay geometry

**Table 2a.** Reconnect model parameters for the A-B (splay) interseam

Reservoir	Mean	Mode	Thickness	Mode	Width	Sinuosity
Thickness	Azimuth	Channel	Thickness	Variation	Width	Variation
m	deg.	%	m	%	m	%
30	170	2	1.26	53	41.6	50
					1.16	28

**Table 2b.** Output statistics for the A-B (splay) interseam

Run	No. Channels	Channel %	% Single Storey	Channel	Channel	Well Connectivity
				Connectivity No.	Connectivity %	
1	13	1	100	9	13	2
2	14	2	100	9	13	1
3	14	2	100	9	12	4
4	14	1	40	9	14	2
5	12	1	50	10	16	2
6	14	1	50	10	13	1
7	14	2	60	9	13	1
8	13	2	95	12	17	1
9	14	1	69	9	13	3
10	13	2	100	10	13	2
Mean	13.5	1.5	76.4	9.6	13.7	1.9

**Table 2c.** Output statistics for the A-B (splay) random replication (Fig. 10b).

<b>Run</b>	<b>No. Channels</b>	<b>Channel %</b>	<b>Channel Connectivity No.</b>	<b>Channel Connectivity %</b>	<b>Well Connectivity</b>
3	18	2	7	11	1

**Table 3.** B-C interseam modeling results, modeled with a splay geometry

**Table 3a.** Reconnect model parameters for the B-C (splay) interseam

Reservoir	Mean	Mode	Thickness	Mode	Width	Sinuosity
Thickness	Azimuth	Channel	Thickness	Width	Variation	Variation
m	deg.	%	m	m	%	Sinuosity %
30	170	17	1.59	41.6	50	28

**Table 3b.** Output statistics for the B-C (splay) interseam

Run	No. Channels	Channel %	% Single Storey	Channel Connectivity No.	Channel Connectivity %	Well Connectivity
1	130	14	14	14	20	44
2	131	16	85	14	20	47
3	130	14	87	14	19	42
4	136	15	84	15	22	51
5	128	14	84	12	20	45
6	132	15	85	18	26	59
7	134	17	82	20	29	47
8	130	15	82	16	24	44
9	123	15	85	14	20	40
10	128	15	83	15	21	42
Mean	130.2	15	77.1	15.2	22.1	46.1

**Table 3c.** Output statistics for the B-C (splay) random replication (Fig. 11).

<b>Run</b>	<b>No. Channels</b>	<b>Channel %</b>	<b>Channel Connectivity No.</b>	<b>Channel Connectivity %</b>	<b>Well Connectivity</b>
2	141	15	15	20	53

**Table 4.** B-C interseam modeling results, modeled with a distributary geometry

**Table 4a.** Reconnect model parameters for the B-C (distributary) interseam

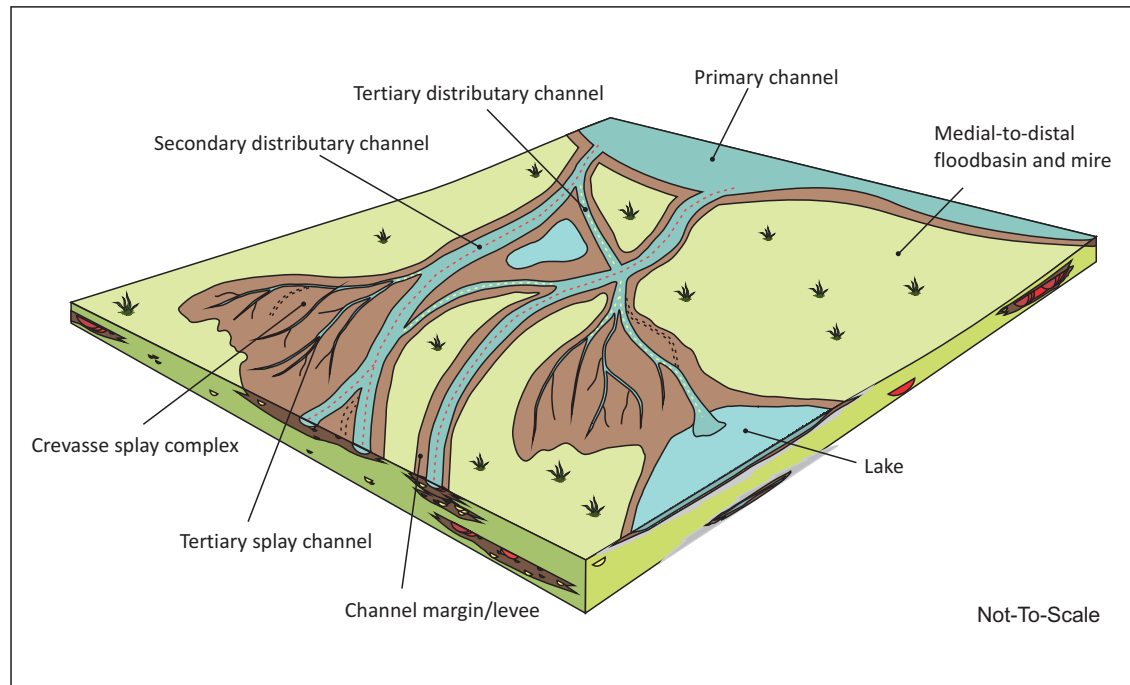
Reservoir Thickness m	Mean Azimuth deg.	Channel %	Mode Thickness m	Thickness Variation %	Mode Width m	Width Variation %	Sinuosity	Sinuosity Variation %
30	170	17	1.59	40	59.8	50	1.3	28

**Table 4b.** Output statistics for the B-C (distributary) interseam

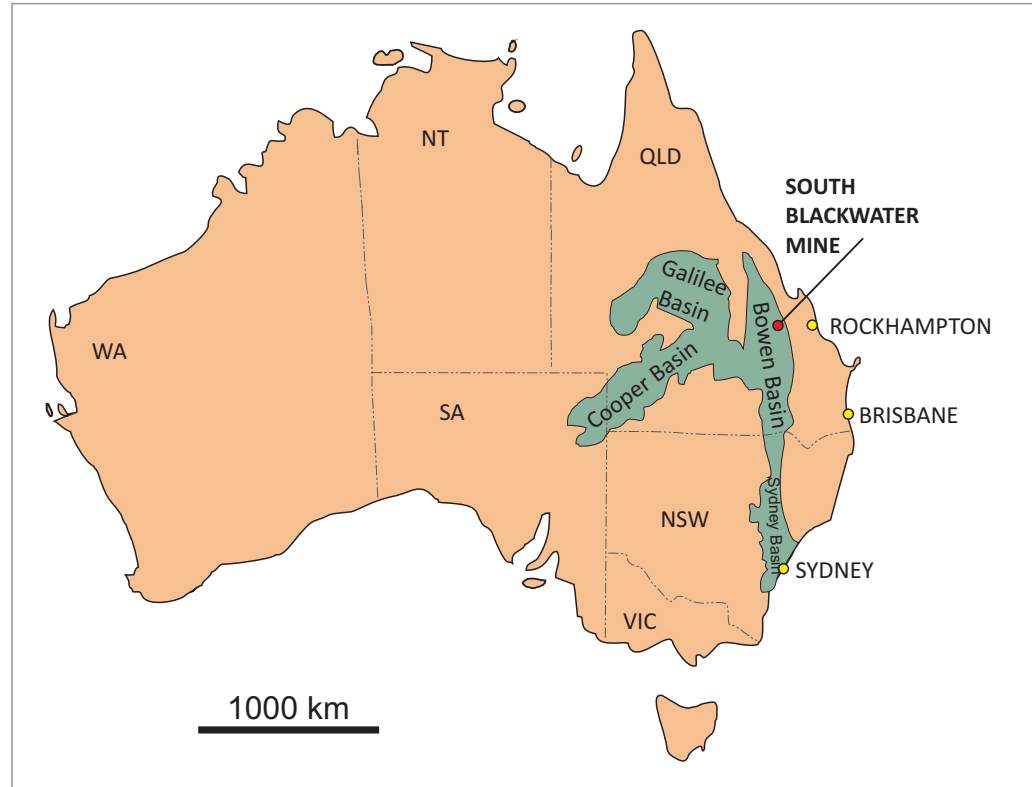
Run	No. Channels	Channel %	% Single Storey	Channel Connectivity No.	Channel Connectivity %	Well Connectivity
1	90	15	86	38	43	83
2	94	17	84	63	68	88
3	89	15	84	51	57	80
4	89	14	90	42	48	74
5	96	17	83	51	54	83
6	90	16	86	43	45	71
7	87	16	85	43	47	80
8	98	17	79	64	70	85
9	94	15	83	45	52	77
10	93	16	82	52	59	77
Mean	92	15.8	84.2	49.2	54.3	79.8

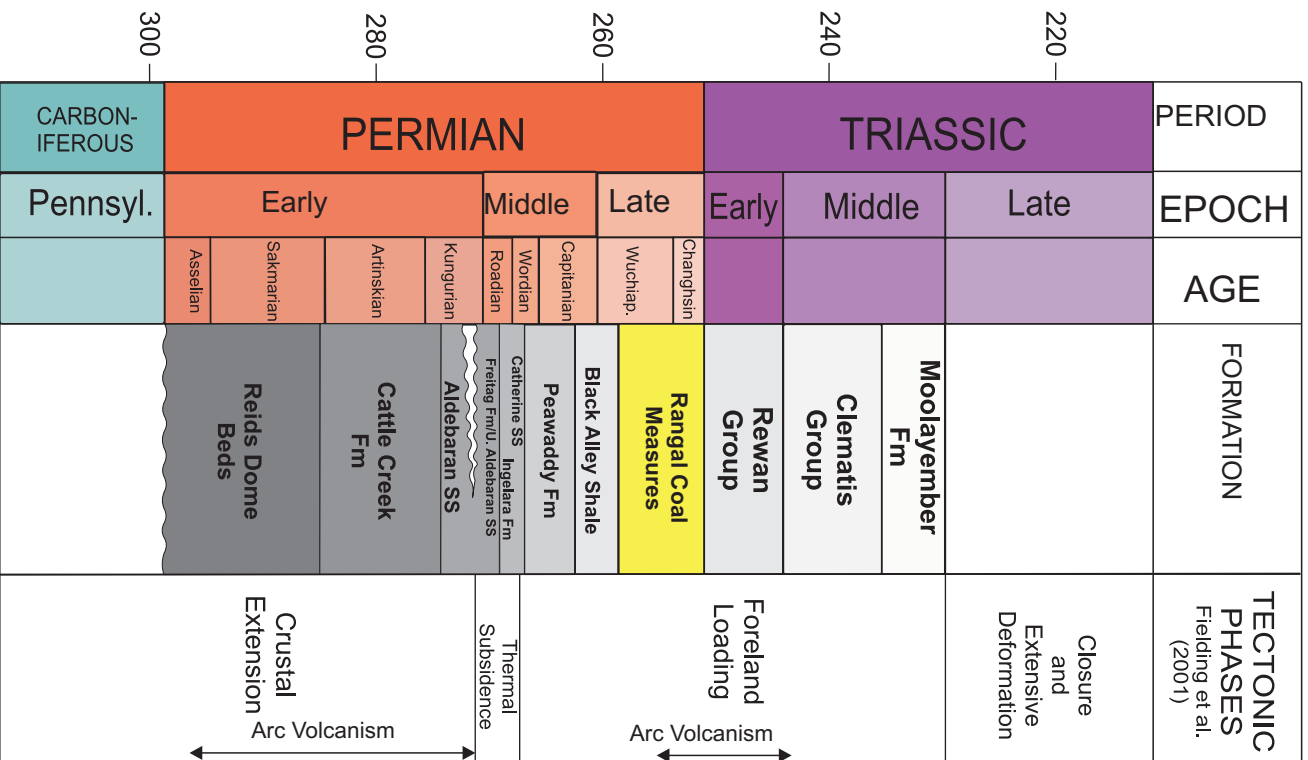
**Table 4c.** Output statistics for the B-C (distributary) random replication (Fig. 12).

<b>Run</b>	<b>No. Channels</b>	<b>Channel %</b>	<b>Channel Connectivity No.</b>	<b>Channel Connectivity %</b>	<b>Well Connectivity</b>
1	92	12	39	45	77



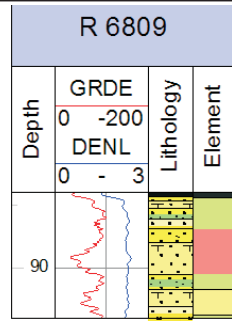






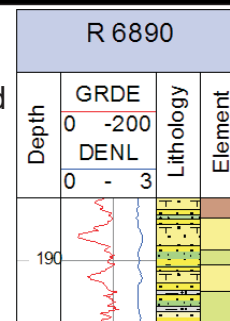
### Secondary Channel

- >3 m-thickness sandstone
- Sharp/erosional base
- Fining-up
- Blocky or bell-shaped gamma response
- <90 API GR



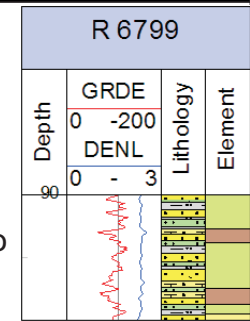
### Tertiary Channel

- <3 m-thickness sandstone
- Typically sharp-based
- Fining-up to clayey, silty-sandstone
- Squat, blocky or bell-shaped gamma response
- <110 API GR



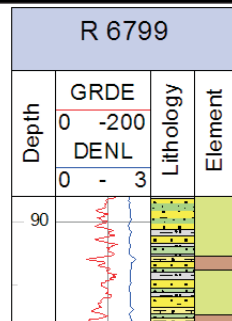
### Channel/Lake Margin

- Interbedded sandstones and siltstones with claystone drapes
- Prograding (coarsening-up) log signature attributed to levees and crevasse splay deposits



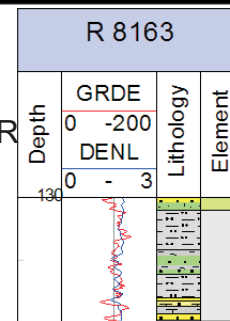
### Proximal-Medial Floodplain

- Interlaminated sandstone, claystone and clay-rich partings
- Highly variable log pattern attributed to splays and flooding



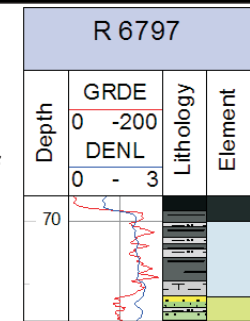
### Distal Floodplain

- Laminated siltstones and mudstones
- GR log signature generally >110 API GR
- Minor sandstones attributed to distal crevasse splays



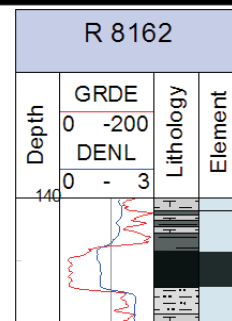
### Lake

- Interlaminated claystones, mudstones and silty mudstones
- Occasional lenses of siltstone and sandstone
- >110 API GR



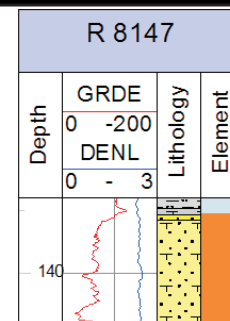
### Mire

- Coals formed in peat mires
- Blocky, low GR log signature in good quality coals
- Low DENL response distinguishes coal from sandstone



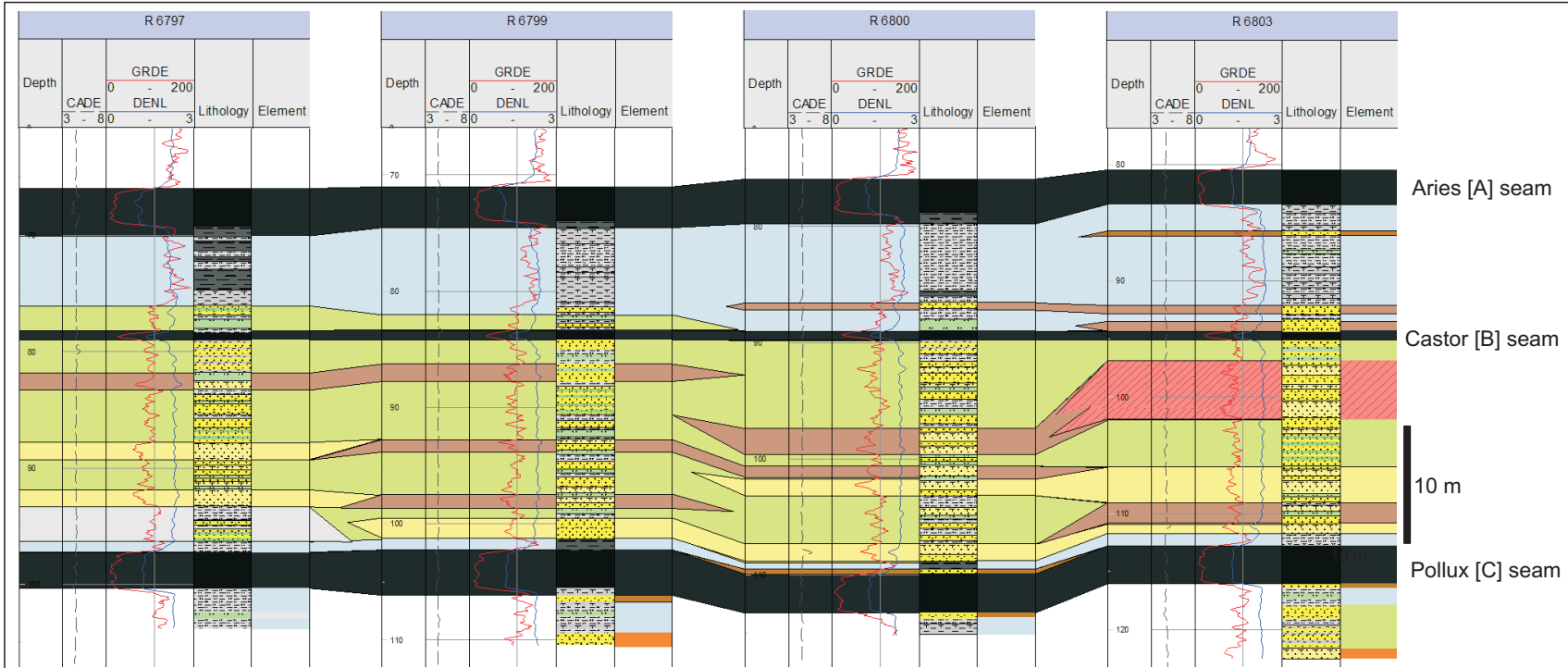
### Primary Channel

- Not seen in the A-C interseam
- Blocky, fining-up log signature
- <90 API GR
- >6 m-thickness sandstone

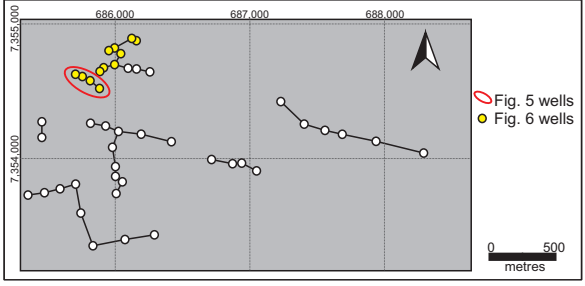


### Key

- Secondary Distributary Channel
- Tertiary Crevasse/Distributary Channel
- Channel Margin/Lake Margin
- Proximal-Medial Floodplain
- Distal Floodplain
- Lake/Frequently Inundated Floodbasin
- Mire
- Sheet-like Fluvial Channel

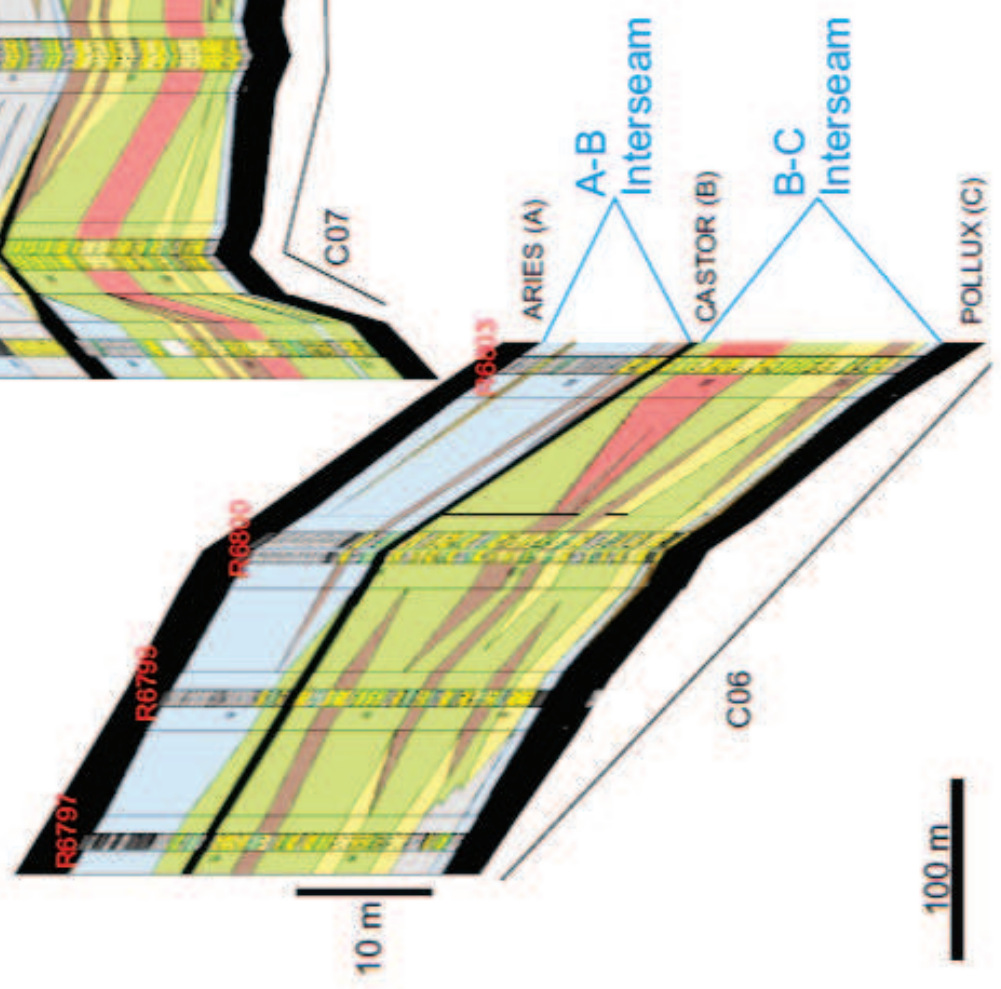
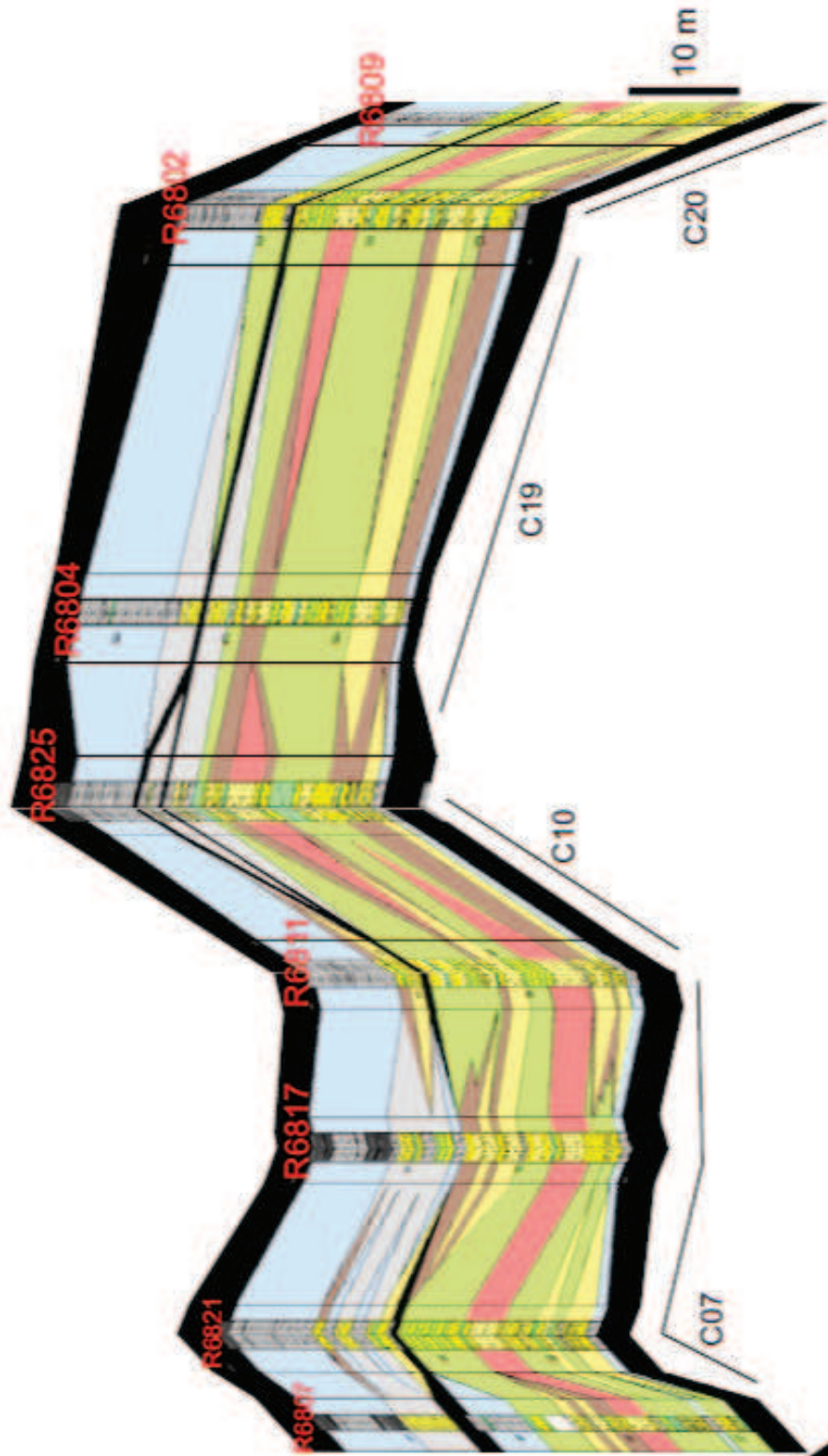


Key		Architectural Element	
<b>Lithology</b>			
	Coal		Facies 1: Sheet-like Fluvial Channel
	Carbonaceous Shale		Facies 2: Heterolithic Distributary Channel
	Mudstone		Facies 3: Minor Crevasse Channel
	Silty Mudstone		Facies 4: Channel Margin/Lake Margin
	Siltstone		Facies 5: Proximal-Medial Floodplain
	Silty Sandstone		Facies 6: Distal Floodplain
	Sandstone		Facies 7: Lake/Frequently Inundated Floodplain
	Cave, no data		Facies 8: Mire
			Facies 9: Overbank Coarser Flood Deposits
			Facies 3a: Stacked Crevasse Channel/ Distributary Channel



Scale (between well panels) **100 m**

Fig. 5 wells  
 Fig. 6 wells

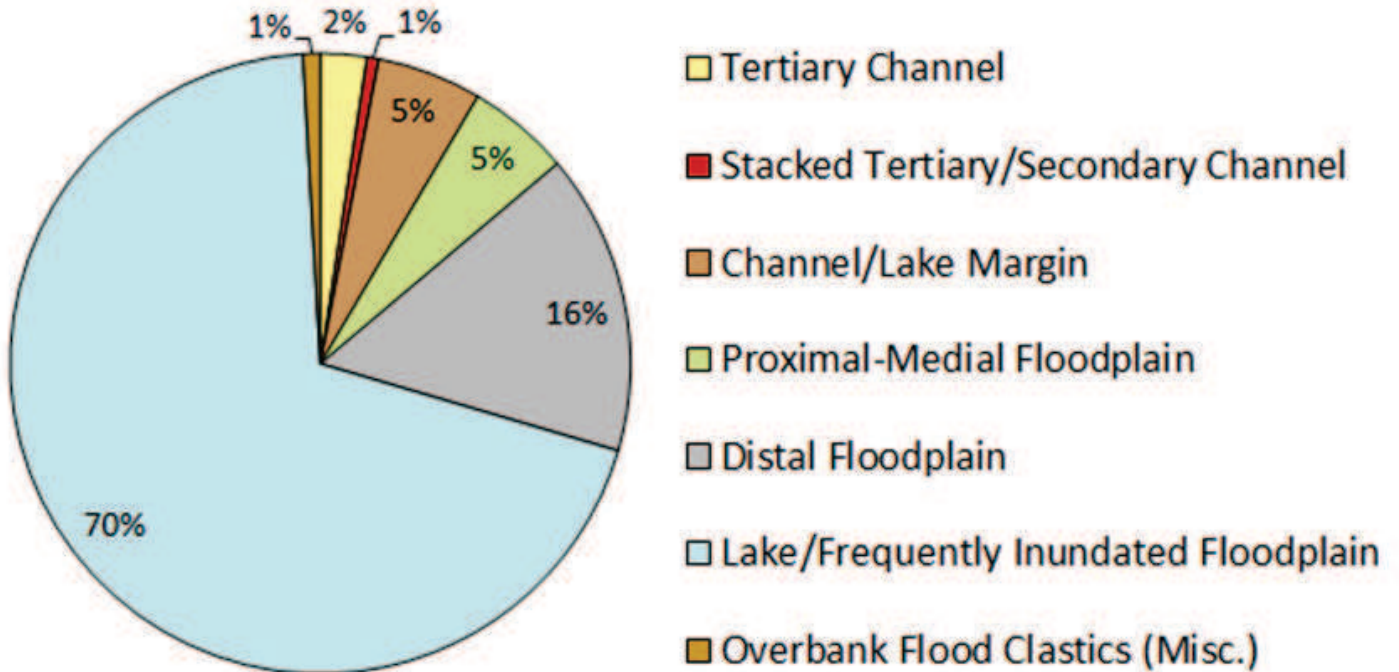


Key	
<b>Lithology</b>	
	Coal
	Carbonaceous Shale
	Mudstone
	Silty Mudstone
	Siltstone
	Silty Sandstone
	Sandstone
	Cave, no data

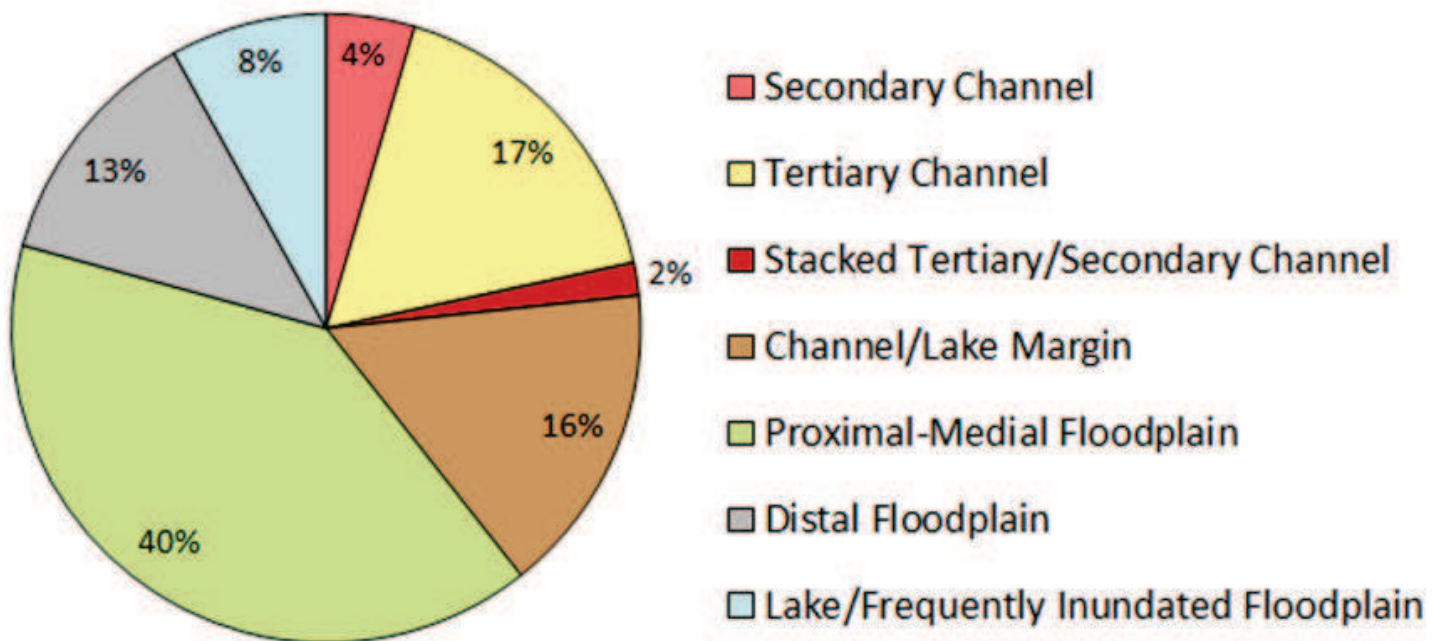
  

Architectural Element	
	Facies 1: Sheet-like Fluvial Channel
	Facies 2: Heterolithic Distributary Channel
	Facies 3: Minor Crevasse Channel
	Facies 4: Channel Margin/Lake Margin
	Facies 5: Proximal-Medial Floodplain
	Facies 6: Distal Floodplain
	Facies 7: Lake/Frequently Inundated Floodplain
	Facies 8: Mire
	Facies 9: Overbank Coarser Flood Deposits
	Facies 3a: Stacked Crevasse Channel/Distributary Channel

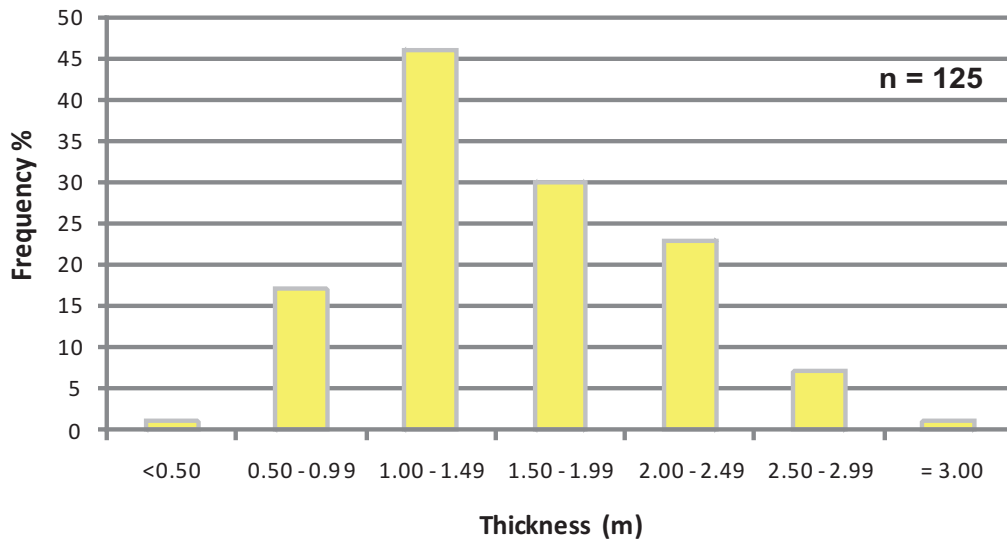
**a. Proportions of Architectural Elements in the A-B interseam interval of the Rangal Coal Measures**



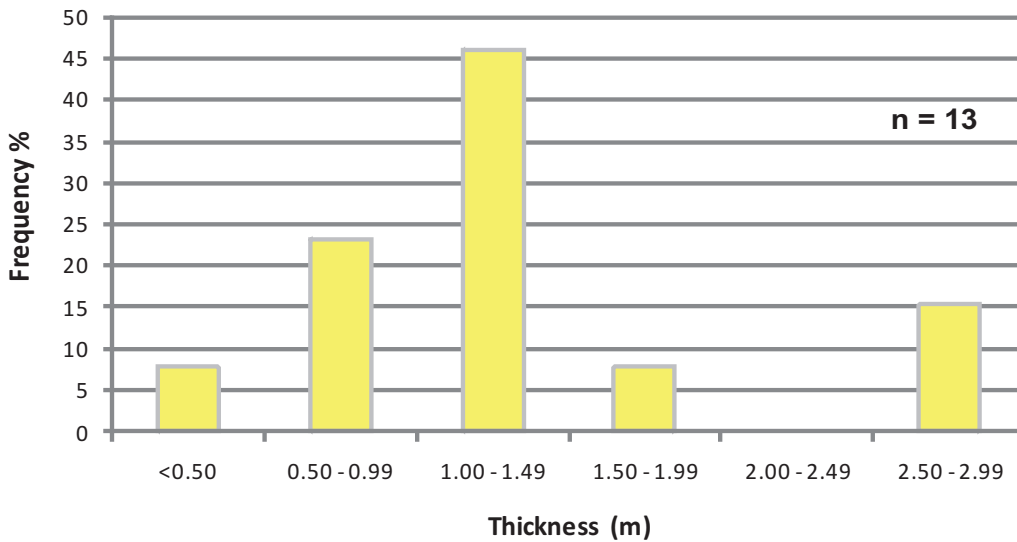
**b. Proportions of Architectural Elements in the B-C interseam interval of the Rangal Coal Measures**



**B-C (Castor-Pollux) Interseam Tertiary Channel Body Thickness Distribution**



**A-B (Aries-Castor) Interseam Tertiary Channel Body Thickness Distribution**



Ob River, Overview

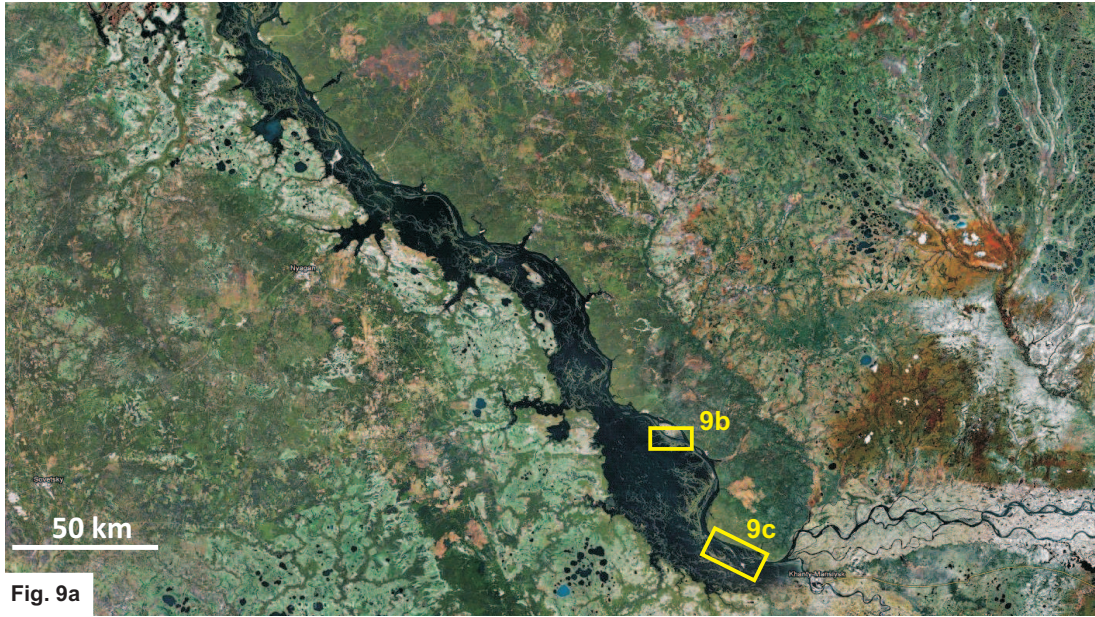


Fig. 9a

Ob River, Splay Analogue

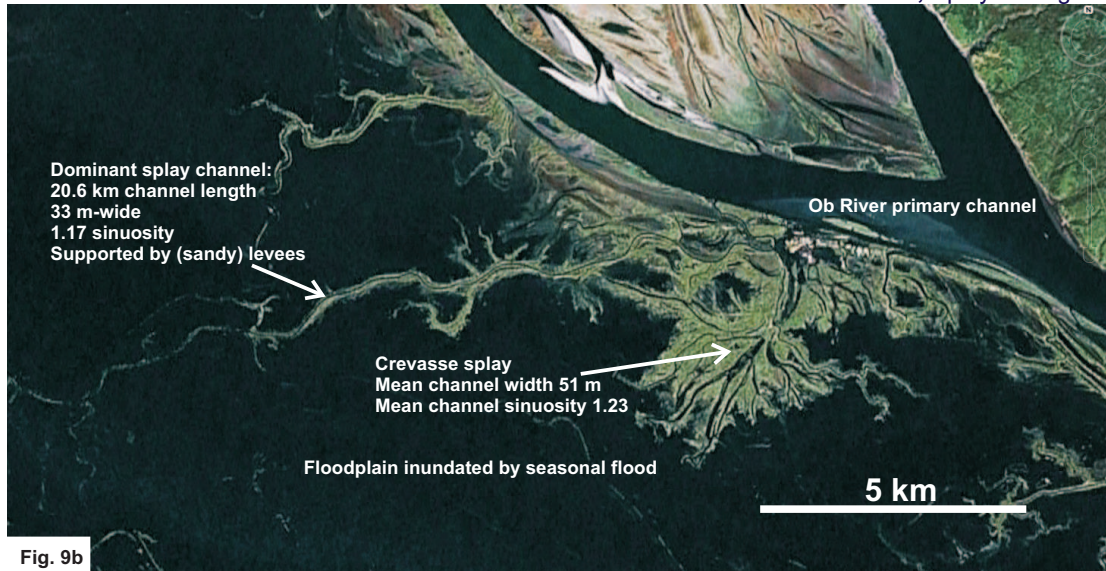


Fig. 9b

Ob River, Distributary Analogue

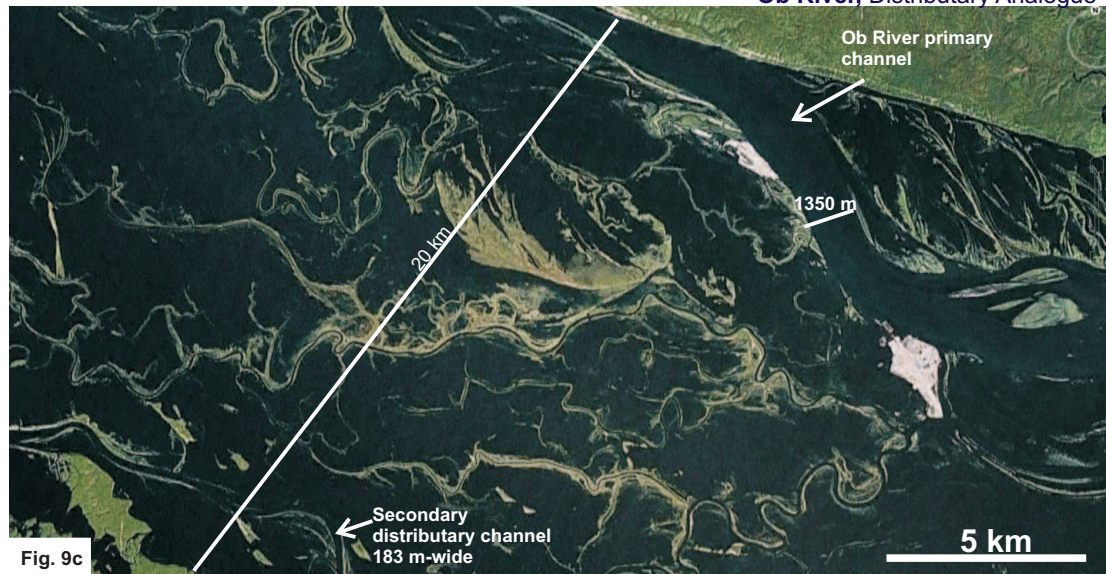
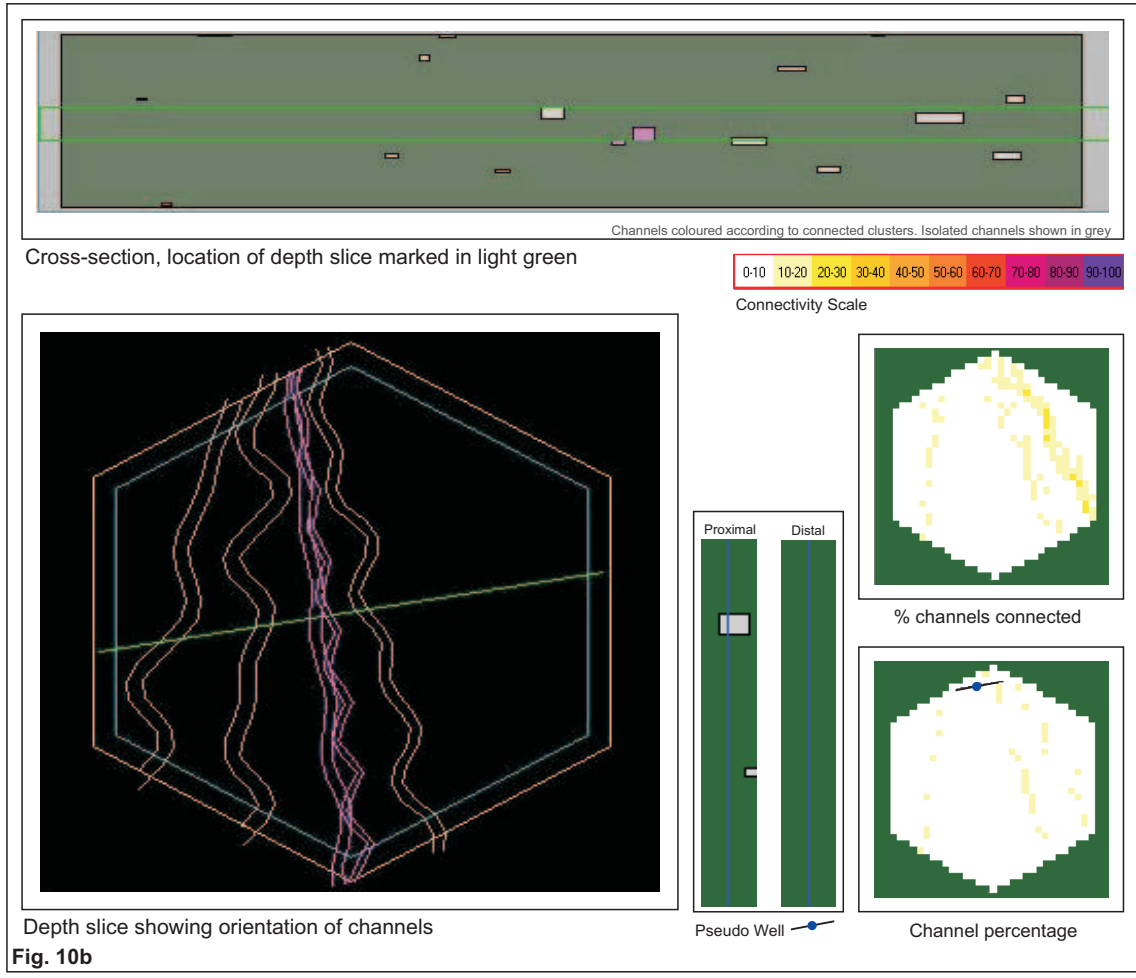
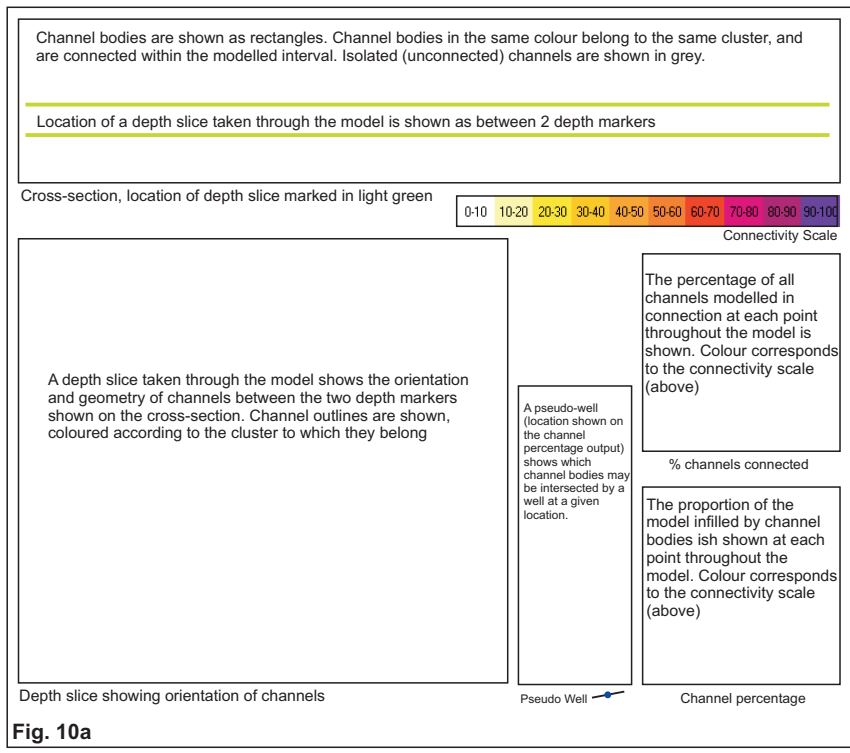
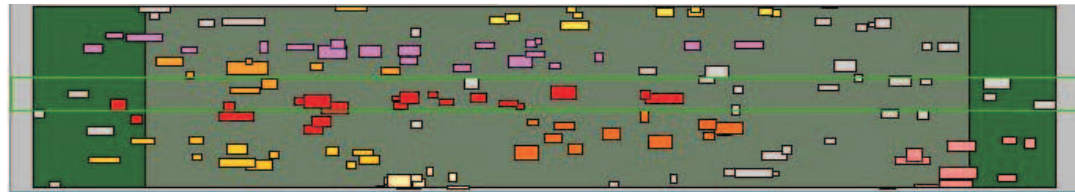


Fig. 9c

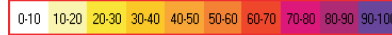




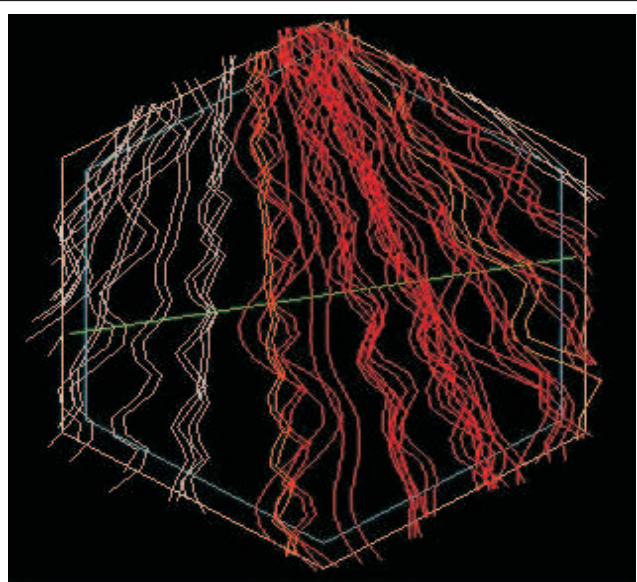


Channels coloured according to connected clusters. Isolated channels shown in grey

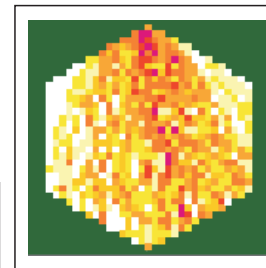
Cross-section, location of depth slice marked in light green



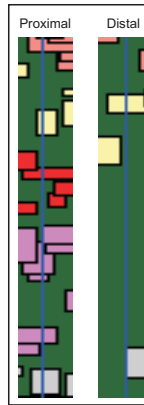
Connectivity Scale



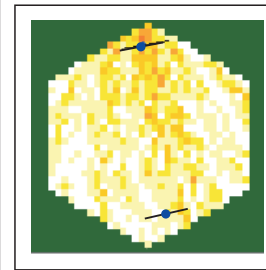
Depth slice showing orientation of channels



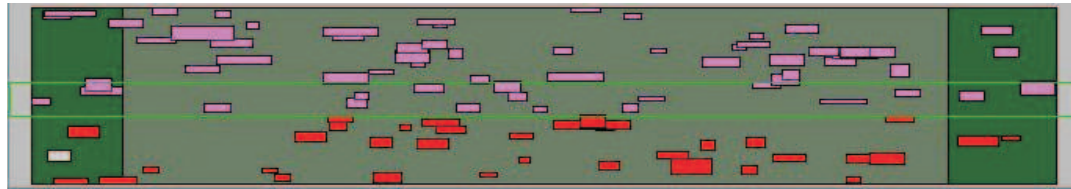
% channels connected



Pseudo Well

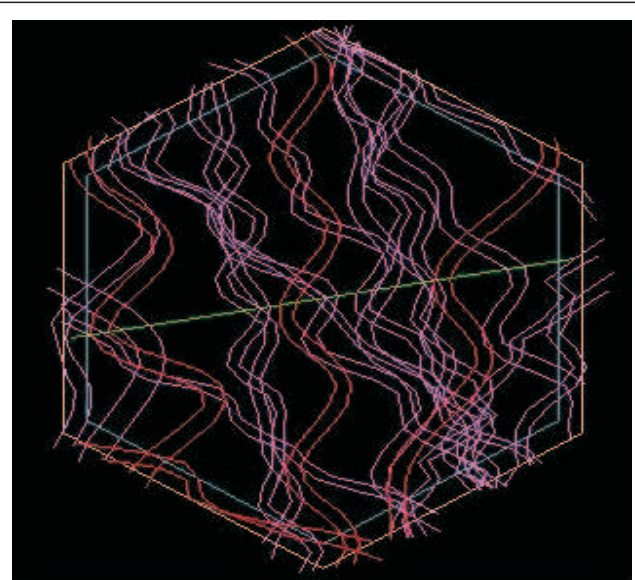
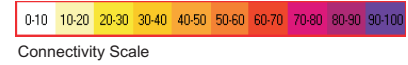


Channel percentage

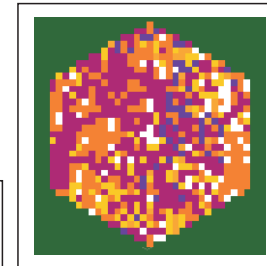


Channels coloured according to connected clusters. Isolated channels shown in grey

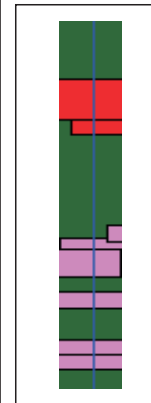
Cross-section, location of depth slice marked in light green



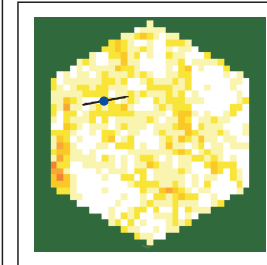
Depth slice showing orientation of channels



% channels connected

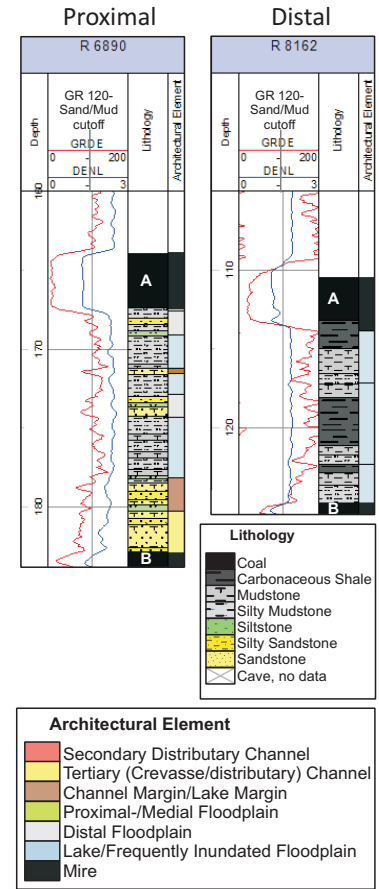
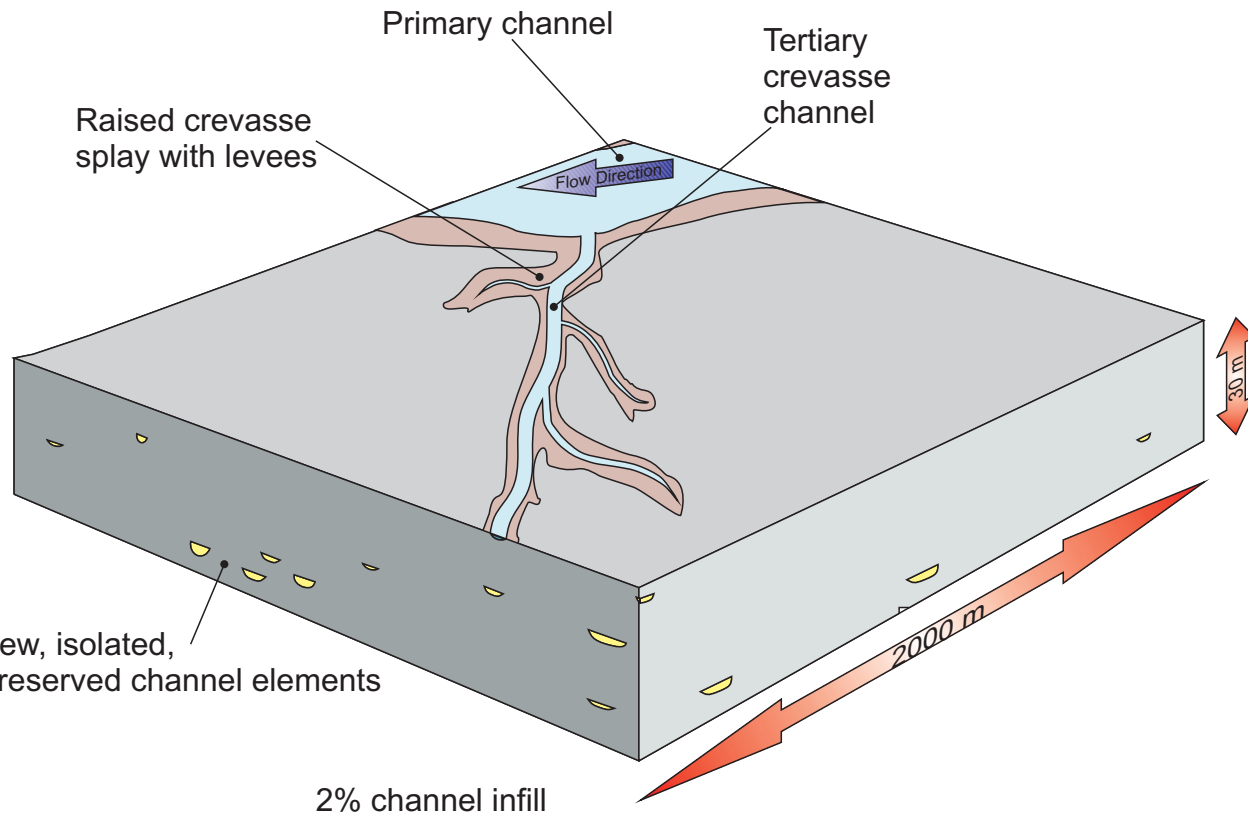


Pseudo Well

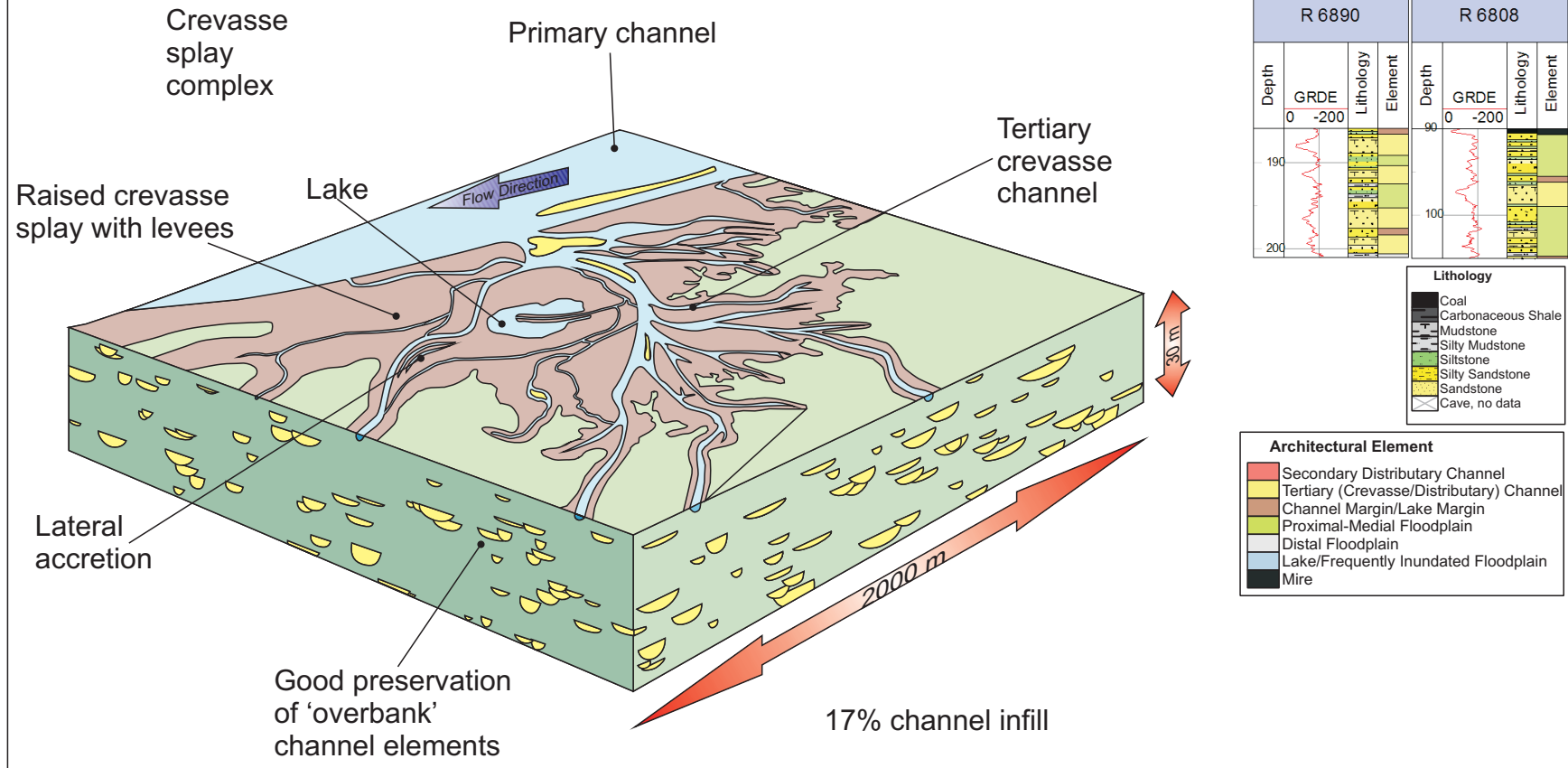


Channel percentage

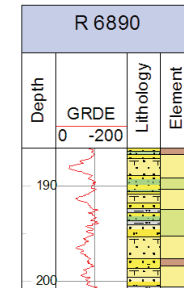
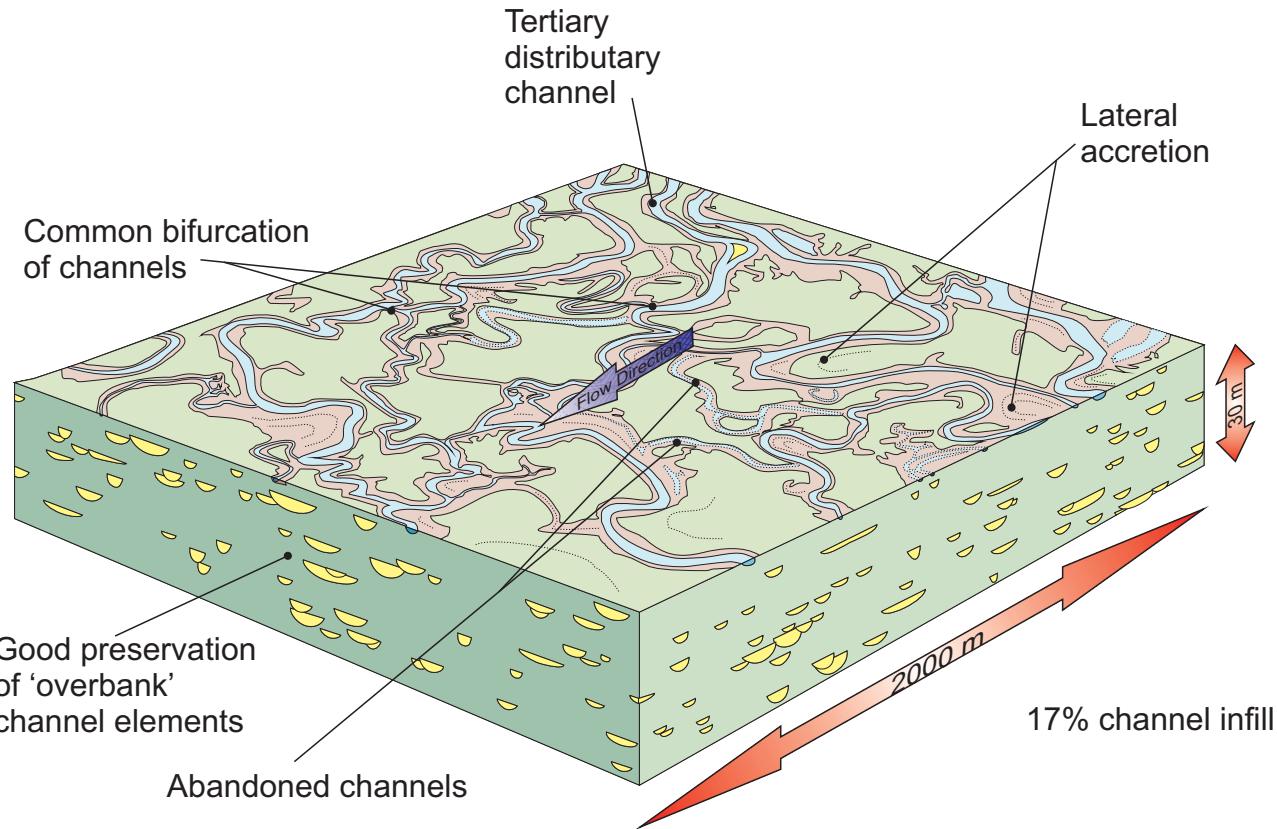
**A-B Interseam,  
Splay Geometry**



## B-C Interseam, Splay Geometry



**B-C Interseam,  
Meandering, Bifurcating Distributary Channels**



**Lithology**

Coal
Carbonaceous Shale
Mudstone
Silty Mudstone
Siltstone
Silty Sandstone
Sandstone
Cave, no data

**Architectural Element**

Secondary Distributary Channel
Tertiary (Crevasse/Distributary) Channel
Channel Margin/Lake Margin
Proximal-Medial Floodplain
Distal Floodplain
Lake/Frequently Inundated Floodplain
Mire